universität wien

DIPLOMARBEIT / DIPLOMA THESIS

Titel der Diplomarbeit / Title of the Diploma Thesis

„Assessment of affinity and selectivity of novel norepinephrine transporter ligands – a binding study “

verfasst von / submitted by

Stefanie Foltin

angestrebter akademischer Grad / in partial fulfilment of the requirements for the degree of

Magistra der Pharmazie (Mag.pharm.)

Wien, 2018 / Vienna, 2018

Studienkennzahl lt. Studienblatt / degree programme code as it appears on the student record sheet:	A 449
Studienrichtung lt. Studienblatt / degree programme as it appears on the student record sheet:	Diplomstudium Pharmazie

Acknowledgement

I would like to express special gratitude to o. Univ.-Prof. Mag. Dr. Helmut Viernstein for the supervision and facilitation of this thesis at the department of pharmaceutical technology and biopharmaceutics.

Thanks are also due to Prof. PD Mag. Dr. Markus Mitterhauser for the provision of the topic of this investigation and the opportunity for the work in the department of radio pharmacy in general hospital Vienna (AKH).

The lectures at university and the labour in the laboratory displayed just an introduction to radiopharmaceuticals. That is the reason, why I really appreciate the possibility of this research – that is not to be taken for granted.

I would like to show appreciation to Dr. Christina Rami-Mark for her support during the time of study and her “helping hand” in every situation - my honestly respect to her.

Special thanks also to all members at AKH and colleagues, who did their work at the same time.

The very last honour to my whole family: “I am very grateful to have you.”

“Success is not final,

failure is not fatal:

it is the courage to continue that counts.”

Winston Churchill

Excerpted from Churchill by Himself

Table of contents

1 Introduction

1.1 Norepinephrine Transporter NET

"The Norepinephrine transporter (NET) is located in the plasma membrane of noradrenergic neurons, where it functions to take up synaptically norepinephrine (NE)." [1]

Noradrenergic neurons are found in the central nervous system but mostly they are postganglionic-sympathetic; whereas the adrenergic neurons are just located in the central nervous system. [2]

High abundance of noradrenergic cells is in the pons and medulla oblongata, but highest density is found in the locus coeruleus, a nucleus in the lateral formatio reticularis. The axons reach parts of the central nervous system, the spinal cord, cerebellum and cerebrum. [2]

The NET is a sodium-dependent carrier, so that a cotransport of Na^+ and Cl^- is a main part of the uptake of Noradrenalin (Norepinephrine, NE). [3]

This co-transport of sodium with the substrate molecule NE appears as a fundamental feature of all SCL6 transporters, the solute carrier 6 gene family, which includes nine plasma membrane transporters depending on sodium and chloride concentrations. Two Na^+ and one Cl^- ions are exchanged with one substrate at NET and DAT, whereas one K^+ and one Cl^- transfers serotonin at the SERT, while simultaneously an antiport of K^+ and H^+ occurs. [4]

In contrast to NET, DAT is most expressed in the cell bodies of the substantia nigra and ventral tegmental area, whereas the expression of SERT is located at the median and dorsal raphe nuclei. As a monoamine membrane protein, the norepinephrine transporter is not only responsible for reuptake of Noradrenalin, but also to a lower extent involved for reuptake of Dopamine, although, the two neurotransmitters do not share an identical chemical structure. This special function, uptake of two diverse types of transmitters, presents the NET as an interesting target structure. [5]

The reuptake of almost 90% of the Norepinephrine complete the essential function of the Norepinephrine transporter as a recycling step.

The retrieval of NE into the vesicles arises through the vesicular monoamine transporter (VMAT), a selective carrier, located on the neuronal membrane, for NE.

The extraneuronal monoamine transporter (EMT) shows off as a more non-selective transporter for NE-reuptake, seeing that Epinephrine and Isoprenalin equally follow the gradient of reuptake. [6]

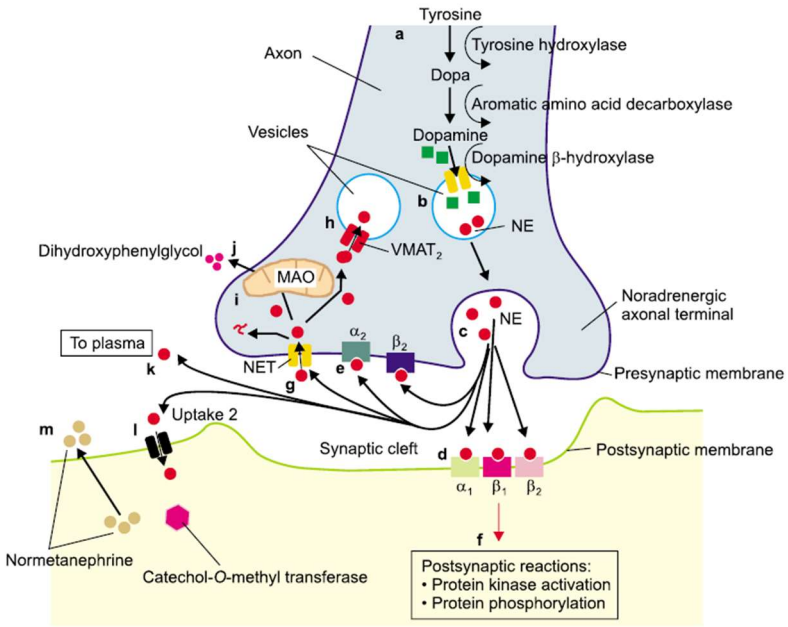

Figure 1: Noradrenergic axon [1]

1.2 Norepinephrine

Norepinephrine (NE) is a classical autonomic transmitter in the mammalian body and is released by sympathetic post-ganglionic nerve terminals and synapses of the central nervous system. It is responsible for many patho- physiological effects on the heart, brain, vessels and others (see following text).

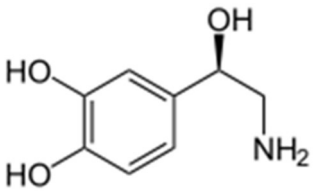

Figure 2: Chemical structure of NE

Its structure represents a benzene ring, two hydroxyl groups and an amino-ethyl chain hydroxylated (see fig.3), the full chemical name is 4-[(1*R*)-2-Amino-1-hydroxyethyl]benzen-1,2-diol (IUPAC). Subsequently, it is an endogenic carrier – a catecholamine - based on the synthesis of the catecholamine cascade, starting with the amino acid Tyrosine, which itself results from Phenylalanine, the smallest aromatic amino acid.

The biosynthesis initiates with a hydroxylation of the precursor L-Tyrosine by Tyrosine hydroxylase to dihydroxyphenylalanine - called DOPA. Tyrosine hydroxylase represents a selective enzyme depending on the chemical structure of the amino acid, its target structure ought to contain a benzene ring, no indol derivatives.

From DOPA to Dopamine, the DOPA decarboxylase pictures the next step of the metabolic way, followed by another unspecific enzyme, the Dopamine-β-hydroxylase, which catalyses the hydroxylation from Dopamine to Norepinephrine. Thus, the final stage of the catecholamines is achieved by the Phenylethanolamine N-methyltransferase (PNMT), it catalyses the synthesis from Norepinephrine to Epinephrine. (see figure 2)

Interestingly, Norepinephrine itself acts as stop modulator of the first biosynthesis step, the catalytic reaction of Tyrosine hydroxylase, so that the synthesis will not end up in an infinite loop. [6]

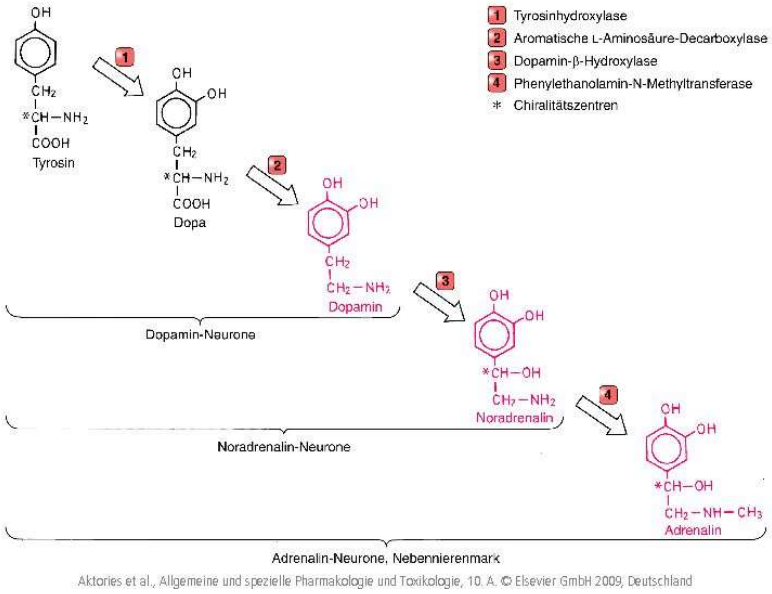

Figure 3: Synthesis of catecholamines [2]

NE is stored in the vesicles (0.3-1.0mol/l) and released by action potentials, depending on the Ca^{+} gradient (shown in Fig.1). The exocytosis of NE out of the vesicles occurs in parallel with the release of small amounts of the Dopamine-β-hydroxylase in a soluble form.

After successful liberation, NE is able to bind on nine adrenergic receptors, which are G-protein coupled: three α_1-adrenergic receptors (α_{1a}, α_{1B}, α_{1D}) $G_{q/12}$-coupled, three α_2 -adrenergic receptors (α_{2a}, α_{2B}, α_{2C}) Gi-coupled and three β-adrenergic receptors (β_1, β_2, β_3) G_s-coupled.

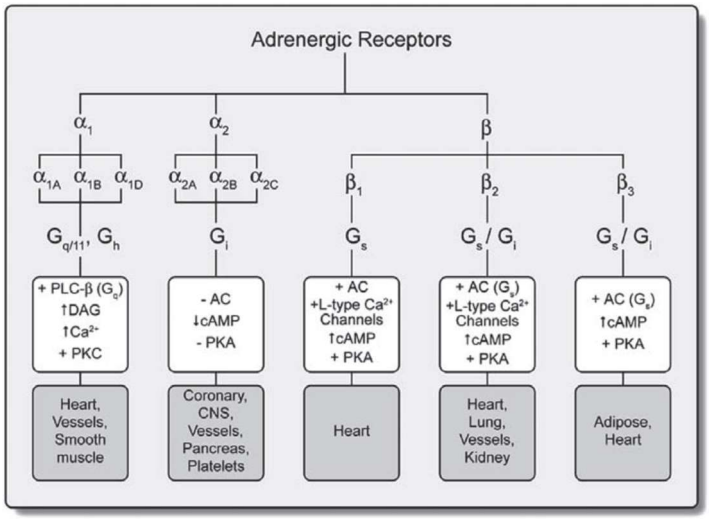

Figure 4: Adrenergic receptor subtypes and their coupled G proteins [7]

Remembering, a G-protein coupled receptor represents a structure of seven transmembrane α-helices, built as a single polypeptide chain, with its N-terminal domain on the extracellular side and the C-term on the intracellular space, which pretends to be the term connected to the G-protein. [6]

Norepinephrine itself exhibits on all adrenergic receptors but β_2-receptor, where Epinephrine is the more active. [2]

Binding of NE to adrenergic receptors can cause several effects including:

- Activation of Phospholipase C/ inositol phosphate system, G_q-coupled
- Activation of Adenylate cyclase/cAMP, G_s-coupled
- Inactivation of Adenylate cyclase/cAMP, G_i-coupled
- Activation of Rho/Rho kinase system, G_{12}-coupled
- Self-inactivation on the α_2-receptor

Due to the producing of cAMP Ca^+ influx occurs, so that another depolarisation follows. The results of depolarisation are more release of NE and its Co-transmitter ATP. [7]

Norepinephrine is metabolised by two enzymes after reuptake to the axoplasm: monoamine oxidase (MAO) and catechol-O-methyl transferase (COMT). The metabolites are aldehydes and are reduced by the aldehyde dehydrogenase. The subsequent metabolic products 3-methoxy-4-hydroxyphenylglycol (MHPG) and 3,4-dihydroxyphenylglycol (DHPG) result from a) the reductive branch in the neurons and vanillylmandelic acid (VAM) and b) 3,4-dihydroxymandelic acid from the oxidative branch of the metabolism. The described metabolic reactions occur in the liver; all by-products pass the urine, where MHPG is the main metabolite. [6]

1.3 Functions of NE

Research targeting functions of Norepinephrine and the Norepinephrine transporter gained increasing interest over the last four decades.

Norepinephrine being a main neuronal component acts as an endogenic hormone of the adrenal medulla, studied as a stress hormone.

By the activation of several α-and β-adrenoreceptors subsequent cascade reactions with significant physiological effects take place.

In the heart action, the effect of NE binding to β_1-adrenergic receptors is resulting inactivation of the sympathetic nervous system, leading to an increase of cAMP. First, as a result on the sinoatrial node, the outcome is the intensifying of the cardiac frequency, namely positive chronotropic. Second, the sympathetic result is positive dromotrope, which means that atrioventricular stimulus conduction is extending. Third, higher cAMP level leads to more force of contraction, called positive inotrope. Consequently, the cardiac output and cardiac oxygen consumption enlarge. [6]

The stimulation of α_1-adrenergic receptors influences all types of smooth muscles, apart from gastrointestinal tract, but especially the vascular part. The α_2-adrenergic receptors affect the smooth muscles, leading to muscle contraction. In contrast, NE action on the β_2-receptors apply relaxation of most smooth muscles by increasing cAMP concentration, in addition to reduce intracellular Ca^+ level, physiological effect is vasodilatation. [6]

The relaxation caused by β_2-adrenoreceptors forces the bronchial dilatation, which shows up as a significant target for the treatment of bronchial diseases like asthma.

Effects in the metabolic system are reported on the one side by the stimulation of α_2-adrenergic receptors formally the inhibition of insulin secretion and on the other side the stimulation of β_3-adrenoceptors as induction of the lipolysis. [6]

1.4 Neuropathophysiological diseases

Increased reuptake of extracellular Norepinephrine in the synapse or an overabundance of Norepinephrine transporters in the Locus coeruleus, can lead to several neuropathophysiological disorders.

1.4.1 Alzheimer`s Disease

Amyloid plaques, neurofibrillary tangles and erosion of neurons demonstrate pathophysiological origins of Alzheimer`s disease (AD). A score of symptoms can be mentioned: neurodegeneration, deficiency in memory and learning, accompanied by aggressive behaviour, depression or hypertension. [6]

There has been evidence that either elevated NE or decreased NETs in LC, or even dysfunction of LC might be factors in case of occurrence of AD. Especially the NET on presynaptically nerve terminals represent a certain role of AD, obviously the number of transporters decrease with human age. The study of Tejani-Butt (1993) reported, that the loss of NET can be measured with the selective marker [^{3}H]-Nisoxetine (NIS). In these studies, the highest density of binding of [^{3}H]-Nisoxetine was found in the LC. The assumption of the decrease of norepinephrine containing cells is evident by the disappearance on binding of [^{3}H]-NIS in AD, which was linked to the loss of neurons in the LC. [8,9]

The assumption that an increasing level of NE itself may cause AD is evaluated by Fitzgerald (2010), who compared numbers of studies considering different coincidences in account to AD. According to that, comorbidities of AD have been evaluated. This study concluded, that the effect of NE on adrenergic receptors and their proximate chain of activation the Ras/MAPK/ERK signalling pathway may enhance the progress of AD. [10]

Pertaining to these assumptions on the influence of NET to AD, a post-mortem autoradiography study with the NET-specific radioligand (S,S)-[^{18}F]FMeNER-D$_2$ showed extraordinary decreases of the amount of NET in the human brain from AD-patients. [11]

1.4.2 Parkinson`s Disease

Hypokinesia, muscle rigidity, tremor or cognitive impairment figure are reported symptoms of Parkinson`s disease. The unique shuffling gait of affected patients force them up to social isolation accomplished with depression, dementia or other autonomic dysregulations. [6]

Pathological changes are the degeneration of dopamine neurons in the substantia nigra and other nerve terminals and also in a smaller extent in NE and 5-HT-rich neurons. According to that, studies with selective agonists and antagonists of adrenergic receptors indicated*," that α_2-receptors are implicated in the control of motor activity and that α_2-receptor antagonists can improve PD motor symptoms …".* [12]

A corroborative argument of the involvement of NE in PD, is the fact that the NET functions to reuptake of DA as well.

1.4.3 Attention Deficit Hyperactivity Disorder

Attention Deficit Hyperactivity Disorder (ADHD), also known its appellation “fidget”, eventuate predominantly before the age of seven years. Significant symptoms are hyperactivity, inattention, impulsivity and cognitive problems in particular: problem solving, planning or working memories.

Prodromal syndromes of ADHD for the diagnosis need to have a persistence of more than six months and a frequent occurrence. [13]

Genetic and environmental basis of ADHD do not sign up an obvious implication of the symptoms. Nevertheless, the evidence of a dysregulation of DA and NE was established by the treatment with methylphenidate hydrochloride (MPH) or atomoxetine (ATX) by blocking of the DAT or NET. Thus, inhibition of the NET by these drugs leads to an increasing of extracellular concentration of DA and NE. [13]

The first PET-investigation with the NET-specific tracer (S,S)-[^{18}F]FMeNER-D_2 did not sign an association of noradrenergic abnormalities in ADHD and non-ADHD patients; however, there is no evidence for exclusion a NE involvement in ADHD unless other brain regions are inspected. [14]

1.4.4 Depression

First mentioned by Schildkraut in 1965, the monoamine structure types as neurotransmitters NE and 5-HT are involved in the initiation of mood disorders.

The reuptake of NE and 5-HT play an emerging role of the invention of antagonists on the receptors to accumulate the transmitters in extracellular space. [6] Perturbated regulation and expression of the norepinephrine transporter in major depression have been prescribed owing to a decline of NET in the locus coeruleus. [15]

"Depression is associated with significant potential morbidity and mortality contributing to suicide, medical illness, disruption of interpersonal relationships, lost work time, and often leading to substance abuse." [16]

Thus, the deficiency of NE leads to lack of concentration, mood instability, low energy or cognitive ability.

The study of Moret et al. explains the assumption, that NE is involved in an outcome of depression:

- innervation of the limbic system from the LC
- dissimilarities between patients with depression and healthy control persons
- genetic mutated mice are inoculated from stress-induced depression
- A rebound-effect to depression after wealthy treatment with NE antidepressant drugs

The noradrenergic therapy with the selective NE reuptake inhibitor like reboxetine or tricyclic antidepressants (TCA) corroborated, that the concentration of NE and DA increased and lead to a regulation of the mood disorder. [16]

1.5 Antagonists and drugs

Due to the large quantity of dissimilar syndromes related to NET perturbations, a variety of drugs have been developed for treatment and also for diagnosis.

Antidepressant drugs like tricyclic antidepressants, SRIs, NRIs or SNRIs are used for the therapy of depression. Their substantial assignment is the supplement of NE or Serotonin transmission due to different mechanism. [17] The adjustment of the NE level is the major step in achieving an effective treatment in depression. [18]

Another group of NET inhibitors were examined by Zhou et al., whose focus laid on the assumption of higher binding effect and selectivity to the NET, due to multiple interactions with the binding sites. Hence, tropane-based and piperidine-based ligands were developed as NET inhibitors and applied in the research of treatment for cocaine abuse, depression or other mental disorders. [1]

In the subsequent subchapters, a selection of relevant NET targeting drugs, currently used in therapy and diagnosis of pathophysiological disorders is presented:

1.5.1 Nisoxetine

(K_i 0.8nM)

[N-methyl-3-(o-methoxyphenoxy)-3-phenylpropylamine], Nisoxetine (NIS) is a potent and selective inhibitor of the uptake of NE with higher affinity to NE than to other monoamines like DA or 5-HT. It was first evaluated as an antidepressant, but further investigations showed up to make NIS as a suitable candidate for use as a radiolabelled compound for measurement of uptake sites for NE. Tejani-Butt characterised [^{3}H]-NIS as a radioligand for quantitation of NE uptake sites by autoradiography or homogenate binding in rat brains. [8]

[^{3}H]-NIS was used as radioligand in this study.

1.5.2 Reboxetine

(K_i 1.1nM)

Reboxetine (RBX) is a Noradrenaline reuptake inhibitor (NRI), showing highly selective binding to NET and thus inhibiting the transporter, and thereby increasing synaptic NE concentration. [19]

The efficacy of RBX was tested, utilizing SDS-PAGE/immune-blotting of tissues of cerebral cortex and other tissues, after a six-week treatment with RBX. The competitive binding assay conducted was done using ^{3}H-nisoxetine (a known NET ligand) and demonstrated a significant reduction of binding. [17]

Miller et al. demonstrated an IC_{50} value of 8.5nM for reboxetine inhibition of uptake of NE. [19] Moreover, RBX is an enantiomer, where the (S,S)-isomer is more potent and selective to NET than the (R,R)-isomer. [20] The distinction of the two enantiomers was evaluated in a molecular dynamics study for the first time, using computational methods for the visualisation of interactions of salt bridge, hydrogen bond and hydrophobic contact between reboxetine and the hot spot residues of the receptor. In conclusion, the (S,S)-enantiomer showed a shorter interaction distance than the (R,R)-enantiomer, so a guarantee of stronger salt bridge and hydrogen bond interaction was obtained. [21]

Consequently, the chemical structure of (S,S)-RBX - a phenoxypropylamine derivative modified with a morpholine-moiety, was chosen as lead structure for development of novel NET inhibitors. [20]

The high affinity at NET was the initial step for the investigation of analogues as potential positron emission tomography (PET) radioligands for the visualisation of the NET. Synthesis and binding assays of new (S,S)-enantiomers were conducted by Zeng et al. Other NET-selective antidepressants (e.g. nisoxetine, desipramine) were excluded for utilization for PET imaging because of their high nonspecific binding. [22]

The progress of reboxetine derivatives is mentioned in point 1.5.3.

In this study reboxetine was used as the compound for the detection of non-specific binding to NET.

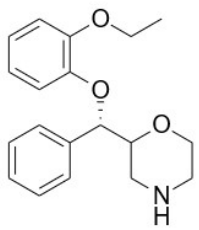

2-((*S*)-(2-ethoxyphenoxy)(phenyl)methyl)morpholine

Figure 5: [S]-enantiomer of reboxetine

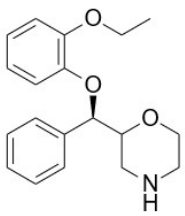

2-((*R*)-(2-ethoxyphenoxy)(phenyl)methyl)morpholin

Figure 6: [R]-enantiomer of reboxetine

1.5.3 (S,S)-[^{18}F]-FMeNER-D$_2$

[(*S,S*)-2-(α-(2-[^{18}F]fluoro[$^{2}H_2$]methoxyphenoxy)benzyl)morpholine] is an analogue of reboxetine, radiolabelled with fluorine-18 and is highly selective to NET. The binding to NET was performed in a study of Takano et al. The imaging of NET with PET was conducted with (S,S)-[^{18}F]-FMeNER-D$_2$.. The specific binding in the thalamus with (S,S)-[^{18}F]-FMeNER-D$_2$ succeeded peak equilibrium during the measurement, by contrast the carbon-11-labelled radioligand [^{11}C]MeNER did not achieve equilibrium, so it was considered to be inappropriate for quantitative analysis. Hence, (S,S)-[^{18}F]-FMeNER-D$_2$ represents a significant PET tracer for NET analysis in living human brain, more selective than different types before.[23]

Consequently, it is used as an imaging biomarker for the surveillance of NET density and quantity in the human brain areas, tested as a potential PET tracer in early detection of AD. [11] Furthermore, a fully-automated synthesis of (S,S)-[^{18}F]-FMeNER-D$_2$ with the precursor (S,S)-NER (=(S,S)-norethyl-reboxetine), originated by the working group of the department of radiochemistry at medical university of Vienna, implies a fast and subsequent working process for clinical use. [24] The clinical study is discontinued.

1.5.4 Tricyclic antidepressants

New medical opportunities in the treatment of depression were opened through the discovery of tricyclic antidepressants in the 1950ies. Their chemical structure is related to the phenothiazines with several tertiary amines, which are derivatised with two methyl groups. Hence, the demethylation to corresponding secondary amines shows up the fast metabolism in vivo. Examples are imipramine, metabolised to desipramine, and amitriptyline degraded to nortriptyline. [6]

Imipramine and clomipramine were used for non-specific binding to NET for the identification of novel SERT tracers in this study.

1.6 Radioligand binding assays

The assessment of new substances, either for therapy or diagnosis, requires well-tried methods. In the PET-imaging research, sensitive tracers for the identification or therapy of neuropathophysiological diseases are in fluently development. Hence, diverse types of binding mechanisms can be used as varieties for preclinical studies.

The binding of a ligand as an agonist on a substrate, leads to an activation of this receptor. In the other case, when an antagonist binds on the receptor, no effect is triggered.

The following binding modes can be observed:

1. Non-competitive binding, special form allosteric binding:

   Ligand A binds to the receptor (A is no substrate on the receptor), so the binding of ligand B may increase or decrease, depending on ligand A.

2. Competitive binding:

   Ligand A and Ligand B compete for the binding site on the same receptor.

The differences among these binding modes play a crucial role in the selection of the way of work, considering whether there are known ligands on the receptor or not.

1.6.1 Competitive binding assays

The ligand binding assay is established in preclinical evaluation on novel drugs. Thus, the procession of competitive binding assays provides a quick and significant insight on an amount of novel substances.

The basis of binding studies, including radioligand investigations, is the law of mass action, representing the ligand and receptor before and after their binding. [25]

$$\text{Ligand} + \text{receptor} \Leftrightarrow [\text{Ligand-receptor}]$$

Conditions of the law of mass action are simultaneously association and dissociation of ligand and receptor until equilibrium achieves, depending on the affinity of the ligand and receptor to each other. The equivalent rate of new ligand-receptor complexes and dissociating ligand-receptor complexes is the determination of equilibrium. [25]

$$[\text{Ligand}] * [\text{Receptor}] * k_{on} = [\text{Ligand-receptor}] * k_{off}$$

The dissociation constant K_d elucidates the concentration of ligand occupying half of the receptors at equilibrium. [25]

$$\frac{[\text{Ligand}] * [\text{Receptor}]}{[\text{Ligand} * \text{Receptor}]} = \frac{koff}{kon} = \text{Kd}$$

The affinity of ligands can be defined per K_d, certainly at equilibrium:

- Small K_d: the receptor has a high affinity for the ligand
- High K_d: the receptor has a low affinity for the ligand

In addition to the K_d values, which are commonly for saturation binding experiments, the K_i concentration is the parallel constant for competition bindings. The testing of several unlabelled compounds, whose affinity to the receptor is unknown, against one concentration of a labelled ligand, whose affinity is determined from pre-studies, is examined trough competition binding tests. Preconditions of these experiments are defined in the variety of concentrations of the unlabelled ligands, e.g. 0.1-1000nM and the confirmed concentration of the radioligand, which needs to have high affinity for not dissociating from the receptor during incubation time. [25]

For the assay, the values of known ligands are reproduced from other studies (Reith et al.), to approve the feasibility of the test set-up.

The compounds are tested by incubation with a defined level of radioligand and membrane until equilibrium is reached. Subsequently, the competition data are

evaluated in a processing (i.e. GraphPad) software and represented as a sigmoid curve. The specific binding (%) on the Y axis is plotted against the logarithm concentrations of the competitor (log[D]) on the X axis.

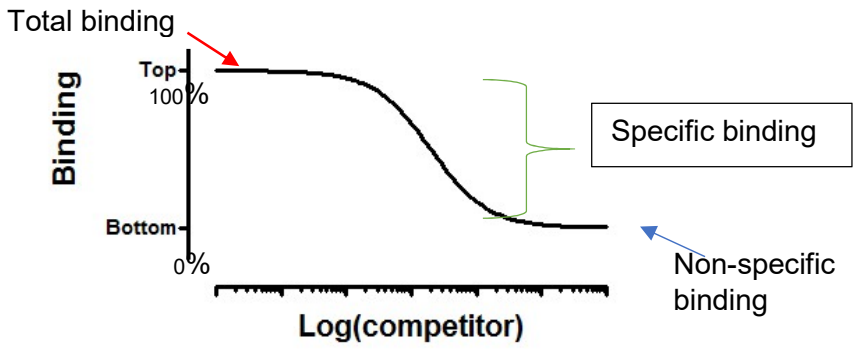

Figure 7: Dose-response curve: competitive binding of tested compounds [25]

The top of the curve demonstrates binding of the radioligand, it is the total binding in the absence of a competitive inhibitor. At the bottom plateau there is the non-specific binding, it shows the entirely block of the receptor with the competitor. The difference between both, is calculated as the specific binding. The applied radioligand concentration is 100nM more than the K_d to the receptor and the concentrations of the unlabelled compound are chosen likewise. [25]

For the calculation of K_i, nonlinear regression is the commonly use to fit the binding curve for the confirmation of the inhibitory concentration IC_{50}. IC_{50} is the concentration of unlabelled drug needed to block 50% of specific binding of the radioligand. Considering that IC_{50} is a value of a presence study, K_i in contrast is a property of the receptor and the unlabelled compound, the following equation of Cheng and Prusoff was used [26]:

$$\mathrm{Ki} = \frac{\mathrm{IC50}}{1 + \frac{[radioligand]}{\mathrm{Kd}}}$$

For the evaluation of results, the Ki values express proportionality to the IC50 values. In conclusion, if the Ki is low, so the affinity to the receptor is high.

1.6.2 Modus operandi of radioligand binding assay

As mentioned above, radioligand binding assays play a fundamental test in the procedure of the development of novel ligands. For the screening of abundant compounds with unknown affinity to the receptor, these assays provide a well-tried method of achieving a small pharmacological profile.

Since the development of binding assays for the SERT, assays became available for DAT and NET recently. [27]

[^{3}H]-Nisoxetine was established as a radioligand for quantitation of NE uptake in 1991 by Tejani et al. [8] From that date, [^{3}H]-NIS has been demonstrated to be used as a radioligand for labelling NE uptake in membranes associated with NET. [28]

The preparation of tissues can be disregarded because the membranes expressing NET are commercially available, assuring high quality standard. The consideration of sufficient affinity of the ligand and specific activity of the radioisotope are prerequisites for suitable radioligand, which is also commercially available. [29]

The incubation of compound, membrane and radioligand is the main part of binding assays to achieve equilibrium of bound and unbound ligand. There is a variety of factors to be mentioned of limiting successfully reactions on the transporter, e.g. incubation time, buffer composition, temperature and pH value. [28,29] The dependence of pH to the equilibrium and the kinetic constant may show an influence of the groups of either the receptor or the ligand, or even the interaction on each other. [29] The electrophysiological site of influence to the binding has been research by Galli et al., especially the effect of the sodium concentration, which *is essential for the steady-state current, it is not for the transient current revealed by DS block.* [4] Despite all, the radioligand concentration is the limiting step of the equilibrium, too less increases the duration.

The separation of the unbound fraction and the receptor-ligand-complex is conducted by rapid vacuum filtration or centrifugation. In this study the Cell Harvester System is the method of operating; the division of free and bound material is performed by quick washing steps, collecting the receptor-ligand-

complex on glass fibre filters. *“Wash times should be optimized to maximize the specific-to-nonspecific ratio.”* [29] Nonspecific binding is higher when the wash times are insufficient so that the radioligand binds on any sites of the receptor or even the filter. To reduce nonspecific binding to the filter, the paper gets pre-soaked in polyethylenimine at a range of 0.1-0.5%. The semi-automated system offers the possibility to testing 36 probes simultaneously. Radioactive and non-radioactive waste is collected separately to decrease costs of decontamination.

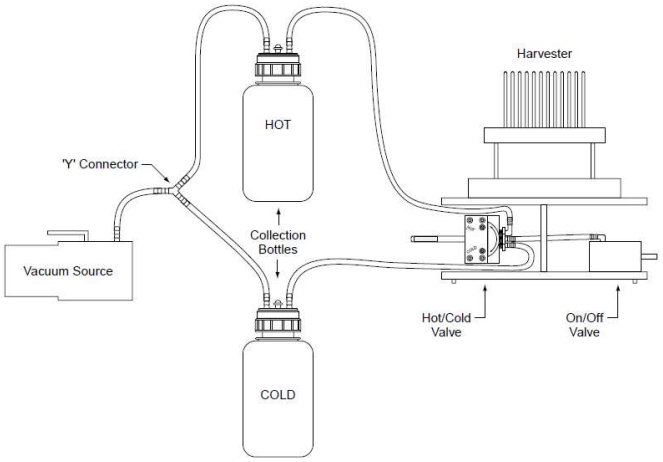

Figure 8: Schema of Brandel® Cell Harvester [30]

For the quantification, the punched-out filter samples are transferred in a vial containing a scintillation cocktail, due to the usage of a tritiated radioligand. For the liquid scintillation counting, Ultima-Gold pretends to be the “Gold standard” reagent for quenching on beta emitting radionuclides like tritium. *“There are two main types of quench: chemical quench occurs during the transfer of energy from the solvent to the scintillator” (...) “and color quench causes attenuation to the photons of light by absorbing and scattering them in the solution…”* As a result, the reduced light output would be available for the measurement by the photomultiplier tubes. [31]

1.7 Radiolabelled measuring with the liquid scintillation counter

For the testing of the affinity of new substances the radioligand binding assay, explained above, has been established over the last decades. Frequently, tritiated radioligands are used, emitting beta radiation.

The quantitative measurement of low-energy beta particles, especially ^{3}H-decay, can be counted with the liquid scintillation method due to the directly contact of the radioactivity with the scintillator. [32]

Tritium is a chemical isotope of hydrogen except of its radioactivity, its half-life is 12.3 years. As a beta particle, it weighs barely a 1/7400 of the mass of an alpha particle; the energy may be deflected very facile. Hence, because of the overabundance of neutrons in the nucleus, two particles – one positron and one negatron – are released. The positron has transient existence and interacts with an electron after expending all its kinetic energy, so that it is “annihilated”. [33] Thus, the positron or alliterated neutrino is not for attraction for the liquid scintillation, except of the small amount of the carried decay energy. However, the negatron, named beta particle, is persistent after expending its energy and “*can possess any energy between 0 and 18.6keV. The energy is kinetic, that is energy of motion.”* [34] This motion is the assignment of the liquid scintillation counting, dissipating in three appearances: heat, ionization and excitation of the molecules. Therefore, a solution – the scintillation cocktail – is delivered to the radiolabelled complex of interest, otherwise the beta particles would dissipate too rapidly. The cocktail is a composition of solvent and solute, so that the excited molecules can be transferred into photons of light, which is the concrete process of detection the radioactivity. The conversion of the energy into photons and the intensity of light is proportional to the forth of the beta molecules. The transformation is depending on the scintillation cocktail and excitation of scintillator molecules. This operation is called quenching, as mentioned above. [34,38]

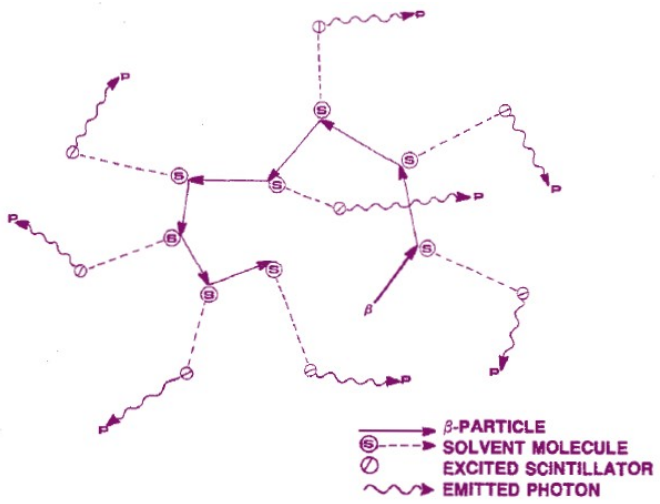

Figure 9: Illustration of the collision process [34]

A photomultiplier tube PMT is used for enhancing the light signal of the photons. The surface of PMT is photosensitive, so that absorbed photons may convert into electrons, which are attracted by the positive potential of an electrode inside the tube for resulting multiplication of electrons, named secondary electrons. In the end, the electrons pass the final electrode creating an electrical pulse, which is proportional to the number of photons, respectively the scintillation events. Modern liquid scintillation counters employ pulse coincidence detection and summation counting, in particular: the signal from one PMT is fed into a circuit of another PMT, so that a circuit occurs which ends in a summation output of all recorded events. This amplification of signals is significant for the further advances in the scintillation technique, the introduction of pulse height energy spectrum analysis. [34,35]

Two aspects of the detection of beta particles, mainly tritium ought to be considered:

1. Beta particles need to have sufficient energy to produce photons to interact with the PMT-surface.
2. The efficiency of the photocathode is not 100% available. The limiting step is the conversion of the photons to electrons. [34,35]

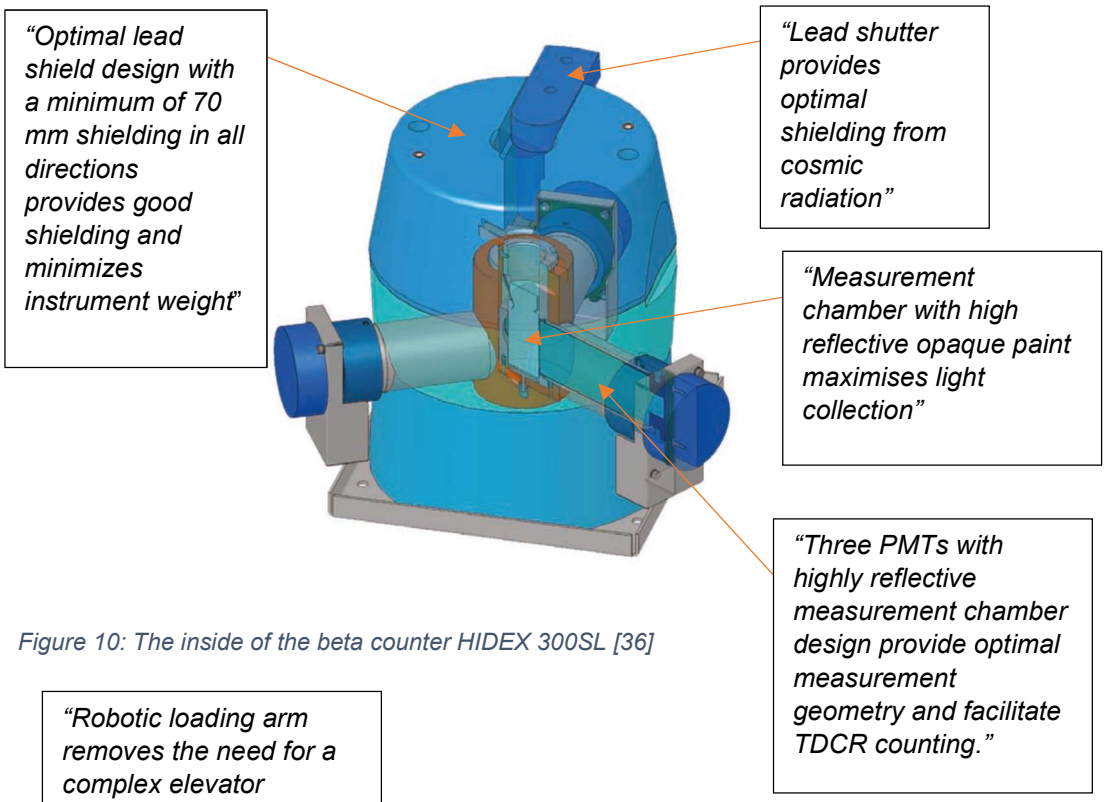

Figure 10: The inside of the beta counter HIDEX 300SL [36]

"Robotic loading arm removes the need for a complex elevator mechanism. Vertical shielding both on top and bottom of detector chambers provides biggest reduction of background effects instrument weight"

2 Aim

“In the central nervous system monoamines, such as norepinephrine (NE, noradrenaline), dopamine (DA) and serotonin (5-HT) play an important role in neurotransmission, so they are involved in various (patho-)physiological functions and processes.” [37]

The intend of this study was to find out some new potential PET-tracers of the Norepinephrine transporter, not based on reboxetine. For that reason, analysis of substances such as FAPPI, PHOXI, DIMAP, MAPPI and HAPTHI are required (these compounds were named during the practical work, their former appellation was a sequence of “VIENET”). The chemical structure varies from benzo[d]imidazolone derivatives, phenoxyisochromen derivatives, indolinyl derivatives, indolinole derivatives and thiadiazole derivatives. The affinity of these targets on each receptor was measured by competition binding assays using the cell harvester method combining a beta-counter and the analysis-system of Graph Pad Prism Software.

For the evaluation of the tracers a compound, such as Reboxetine, which is pharmacologically known as antagonist against NET, was used for the comparison; those for DAT were GBR 12909, for SERT Clomipramine.

The membranes were human NET, human SERT and human DAT. Compounds like FAPPI 1, FAPPI 2 and FAPPI 3 were synthesized at University of Vienna, others like HAPTHI, DIMAP or MAPPI and all their derivatives od VIENET were offered from ABX advanced biochemical compounds, Biomedizinische Forschungsreagenzien GmbH Radeberg, Germany.

After the evaluation of affinity of novel lead structures at NET, studies at DAT and SERT were performed to evaluate their selectivity.

3 Materials and Methods

3.1 Materials

The newly synthesized compounds were provided from the University of Vienna - Department of Pharmaceutical Chemistry Division of Drug Synthesis, such as FAPPI 1, FAPPI 2 and FAPPI 3. All other synthesized substances, like HAPHTI, MAPPI, DIMAP, including their methylated- or fluorethylated-derivatives, were delivered from ABX advanced biochemical compounds, Biomedizinische Forschungsreagenzien GmbH Radeberg, Germany.

Used membrane target systems were human NET (RHBNETM400UA), human SERT (RHBSTM400UA) and human DAT (RHBDATM400UA), all from Perkin Elmer, Boston USA.

The radioactive material for labelling the substances was Nisoxetine Hydrochloride-[N-Methyl-^{3}H] (NET108425UC), WIN 35,428-[N-methyl-^{3}H] (NET576250UC), Imipramine Hydrochloride-[Benzene ring-^{3}H(N)] (NET1033250UC), as well purchased from Perkin Elmer, Boston USA.

Potassium chloride, sodium chloride, Tris(hyrdoxymethyl)aminomethane (TRIS), Ascorbic acid, Polyethylenimin (PEI 50% w/w), Acetonitrile and Ultima Gold (high flash point liquid scintillation cocktail - biodegradable) were purchased from Perkin Elmer, Boston USA.

Vials (“pico hang-in” miniature polyethylene scintillation vials Nr.600186, 6ml) for the scintillation cocktail were traded by Perkin Elmer, test tubes (falcon tube 15 ml high clarity polypropylene conical) for centrifugation and culture tubes (Pyrex® disposable vials, rimless) were applied from Sigma Aldrich.

The filter paper Whatman GF/C was traded by Brandel® Inc., Gaithersburg USA.

Name	Chemical structure	Mw g/mol
FAPPI 1	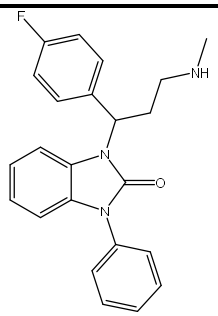 1-(1-(4-fluorophenyl)-3-(methylamino)propyl)-3-phenyl-1,3-dihydro-2 *H*-benzo[*d*]imidazol-2-one Molecular Weight: 375,45	375.45
FAPPI 2	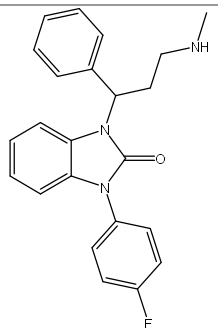 1-(4-fluorophenyl)-3-(3-(methylamino)-1-phenylpropyl)-1,3-dihydro-2 *H*-benzo[*d*]imidazol-2-one Molecular Weight: 375,45	375.45
FAPPI 3	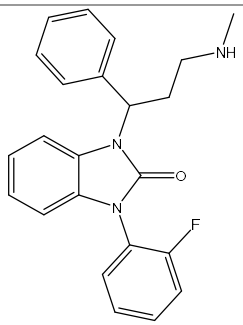 1-(2-fluorophenyl)-3-(3-(methylamino)-1-phenylpropyl)-1,3-dihydro-2 *H*-benzo[*d*]imidazol-2-one Molecular Weight: 375,45	375.45

Table 1: FAPPI

Name	Chemical structure	Mw g/mol
VieNET E0 =PHOXI 1	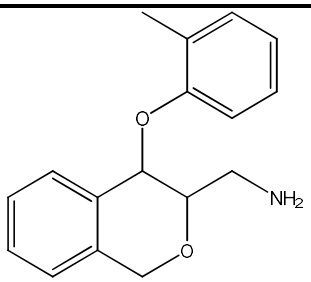 (4-(*o*-tolyloxy)isochroman-3-yl)methanamine Molecular Weight: 257,33	257.33
VieNET E1 =Me@PHOXI1	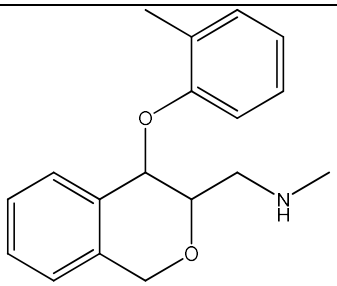 *N*-methyl-1-(4-(*o*-tolyloxy)isochroman-3-yl)methanamine Molecular Weight: 283,36	283.36
VieNET E2 =FMe@PHOXI1	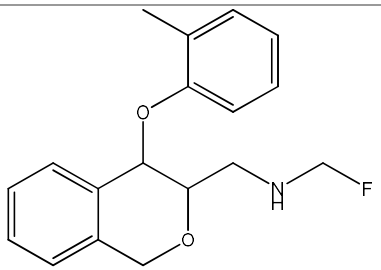 1-fluoro-*N*-((4-(*o*-tolyloxy)isochroman-3-yl)methyl)methanamine Molecular Weight: 301,36	301.36
VieNET E3 =FE@PHOXI1	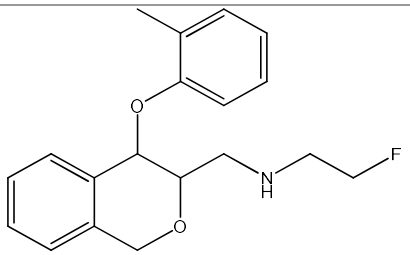 2-fluoro-*N*-((4-(*o*-tolyloxy)isochroman-3-yl)methyl)ethanamine Molecular Weight: 315,38	315.38

Table 2: PHOXI 1

Name	Chemical structure	Mw g/mol
VieNET E4 =PHOXI 2	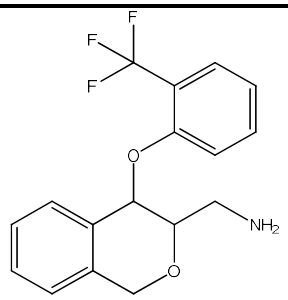 (4-(2-(trifluoromethyl)phenoxy)isochroman-3-yl)methanamine Molecular Weight: 323,31	323.31
VieNET E5 =Me@PHOXI 2	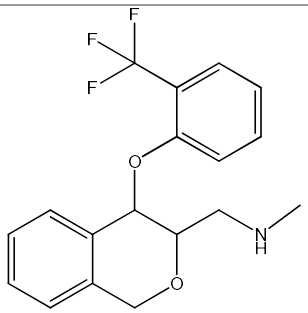 *N*-methyl-1-(4-(2-(trifluoromethyl)phenoxy)isochroman-3-yl)methanamine Molecular Weight: 337,34	337.34
VieNET E6 =FMe@PHOXI 2	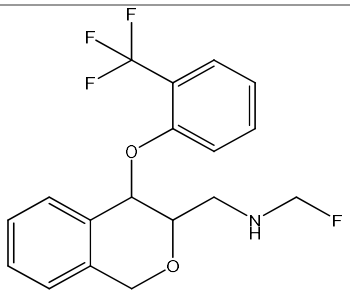 1-fluoro-*N*-((4-(2-(trifluoromethyl)phenoxy)isochroman-3-yl)methyl)methanamine Molecular Weight: 355,33	355.33
VieNET E7 =FE@PHOXI2	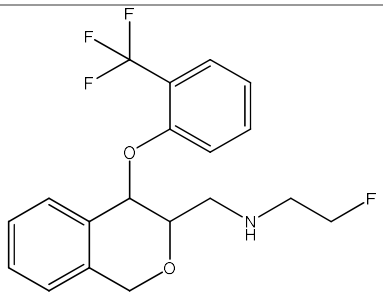 2-fluoro-*N*-((4-(2-(trifluoromethyl)phenoxy)isochroman-3-yl)methyl)ethanamine Molecular Weight: 369,35	369.35

Table 3: PHOXI 2

Name	Chemical structure	Mw g/mol
VieNET E8 PHOXI 3	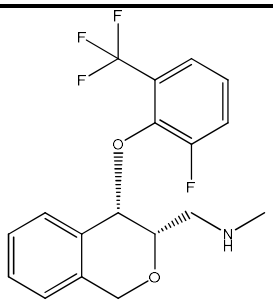 1-((3*S*,4*S*)-4-(2-fluoro-6-(trifluoromethyl)phenoxy)isochroman-3-yl)-*N*-methylmethanamine Molecular Weight: 355,33	355.33
VieNET E9 Me@PHOXI 3	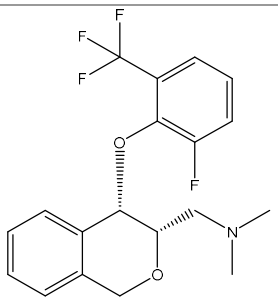 1-((3*S*,4*S*)-4-(2-fluoro-6-(trifluoromethyl)phenoxy)isochroman-3-yl)-*N*,*N*-dimethylmethanamine Molecular Weight: 369,36	369.36
FE@PHOXI 3	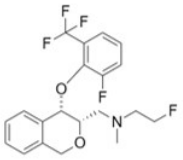 2-fluoro-*N*-(((3*S*,4*S*)-4-(2-fluoro-6-(trifluoromethyl)phenoxy)isochroman-3-yl)methyl)-*N*-methylethan-1-amine Molecular Weight: 401,37	401.37

Table 4: PHOXI 3

Name	Chemical structure	Mw g/mol
VieNET B0 =VIENET 10 DIMAP	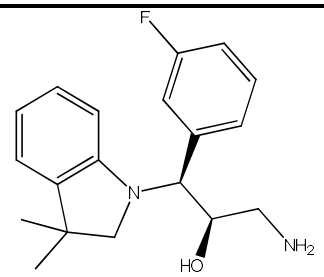 (1*S*,2*R*)-3-amino-1-(3,3-dimethylindolin-1-yl)-1-(3-fluorophenyl)propan-2-ol Molecular Weight: 314,40	314.4
VieNET B1 =VIENET 11 Me@DIMAP	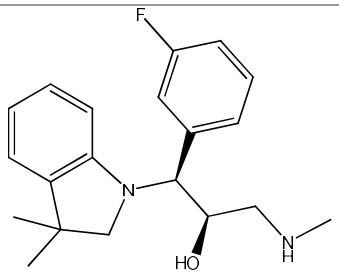 (1*S*,2*R*)-1-(3,3-dimethylindolin-1-yl)-1-(3-fluorophenyl)-3-(methylamino)propan-2-ol Molecular Weight: 328,42	328.42
VieNET B2 FMe@DIMAP	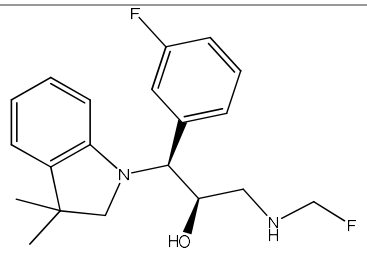 (1*S*,2*R*)-1-(3,3-dimethylindolin-1-yl)-3-((fluoromethyl)amino)-1-(3-fluorophenyl)propan-2-ol Molecular Weight: 346,41	346.41
VieNET B3 =VIENET 13 FE@DIMAP	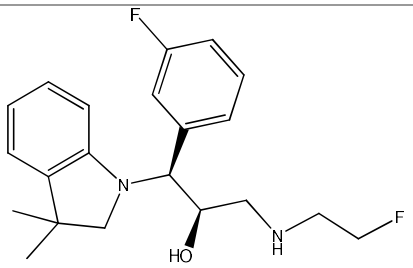 (1*S*,2*R*)-1-(3,3-dimethylindolin-1-yl)-3-((2-fluoroethyl)amino)-1-(3-fluorophenyl)propan-2-ol Molecular Weight: 360,44	360.44

Table 5: DIMAP

Name	Chemical structure	Mw g/mol
VieNET C0 =VIENET 30 MAPPI	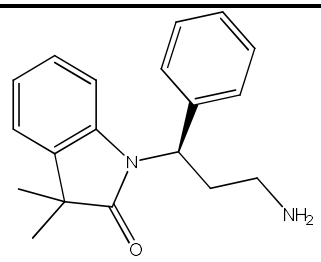 (*R*)-1-(3-amino-1-phenylpropyl)-3,3-dimethylindolin-2-one Molecular Weight: 294,39	294.39
VieNET C1 =VIENET 31 Me@MAPPI	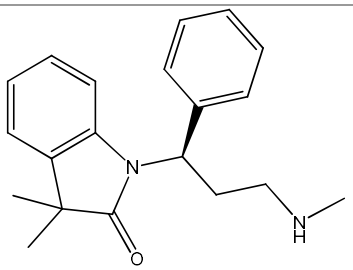 (*R*)-3,3-dimethyl-1-(3-(methylamino)-1-phenylpropyl)indolin-2-one Molecular Weight: 308,42	308.42
VieNET C2 FMe@MAPPI	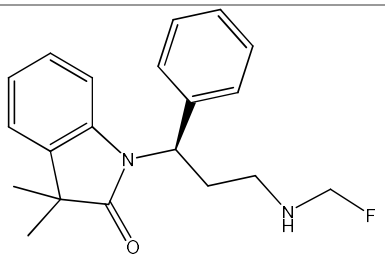 (*R*)-1-(3-((fluoromethyl)amino)-1-phenylpropyl)-3,3-dimethylindolin-2-one Molecular Weight: 326,41	326.41
VieNET C3 =VIENET 33 FE@MAPPI	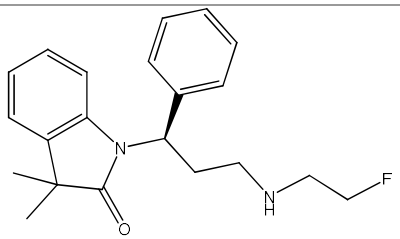 (*R*)-1-(3-((2-fluoroethyl)amino)-1-phenylpropyl)-3,3-dimethylindolin-2-one Molecular Weight: 340,43	340.43
VieNET C4 MeF@MAPPI	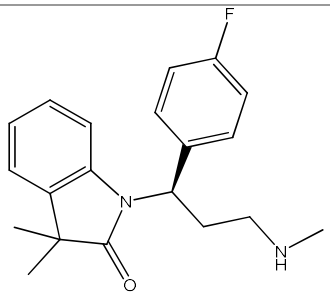 (*R*)-1-(1-(4-fluorophenyl)-3-(methylamino)propyl)-3,3-dimethylindolin-2-one Molecular Weight: 326,41	326.41

Table 6: MAPPI

Name	Chemical structure	Mw g/mol
VieNET D0 =VIENET 20 HAPTHI	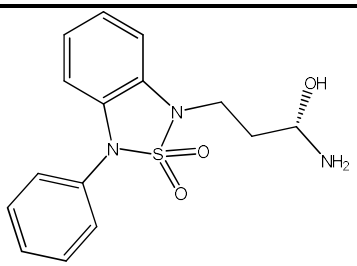 (*S*)-1-(3-amino-3-hydroxypropyl)-3-phenyl-1,3-dihydrobenzo[*c*][1,2,5]thiadiazole 2,2-dioxide Molecular Weight: 319,38	**319.38**
VieNET D1 =VIENET 21 Me@HAPTHI	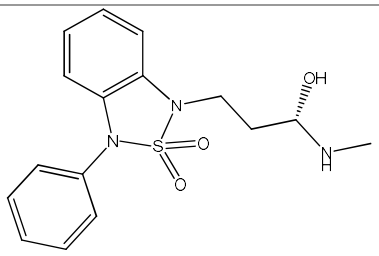 (*S*)-1-(3-hydroxy-3-(methylamino)propyl)-3-phenyl-1,3-dihydrobenzo[*c*][1,2,5]thiadiazole 2,2-dioxide Molecular Weight: 333,41	333.41
VieNET D2 FMe@HAPTHI	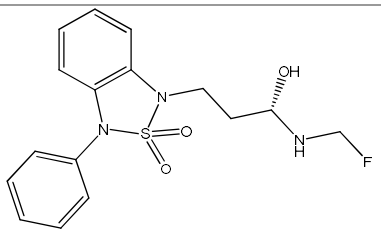 (*S*)-1-(3-((fluoromethyl)amino)-3-hydroxypropyl)-3-phenyl-1,3-dihydrobenzo[*c*][1,2,5]thiadiazole 2,2-dioxide Molecular Weight: 351,40	351.4
VieNET D3 =VIENET 23 FE@HAPTHI	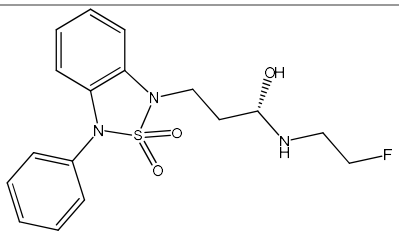 (*S*)-1-(3-((2-fluoroethyl)amino)-3-hydroxypropyl)-3-phenyl-1,3-dihydrobenzo[*c*][1,2,5]thiadiazole 2,2-dioxide Molecular Weight: 365,42	365.42
VieNET D4 MeF@HAPTHI	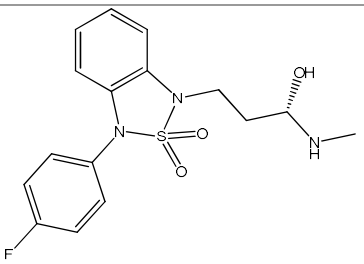 (*S*)-1-(4-fluorophenyl)-3-(3-hydroxy-3-(methylamino)propyl)-1,3-dihydrobenzo[*c*][1,2,5]thiadiazole 2,2-dioxide Molecular Weight: 351,40	351.4

Table 7: HAPTHI

Name	Chemical structure	Mw g/mol
NER	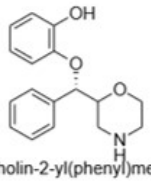 2-((1*S*)-morpholin-2-yl(phenyl)methoxy)phenol Molecular Weight: 285,34	285.34
Reboxetine	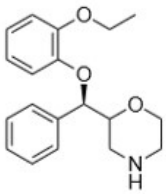 2-((*R*)-(2-ethoxyphenoxy)(phenyl)methyl)morpholine Molecular Weight: 313,40	313.40
Nisoxetine	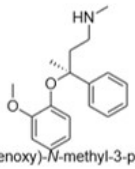 (*S*)-3-(2-methoxyphenoxy)-*N*-methyl-3-phenylbutan-1-amine Molecular Weight: 271,36	271.36
Me@APPI	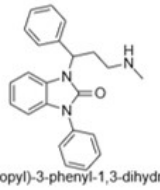 1-(3-(methylamino)-1-phenylpropyl)-3-phenyl-1,3-dihydro-2*H*-benzo[*d*]imidazol-2-one Molecular Weight: 357,46	357.46
Imipramin	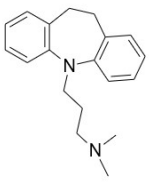 3-(10,11-dihydro-5*H*-dibenzo[*b*,*f*]azepin-5-yl)-*N*,*N*-dimethylpropan-1-amine	280.404

Table 8: References

3.2 Apparatus: Cell Harvester

The usage of the cell harvester method has been well-tried for receptor characterisation and assessment of affinity of new substances. This work was practised with a M-36 tygon tubed Cell harvester (Brandel®, Gaithersburg, USA) using Whatman GF/C filters. For analysis of the successful binding of the material a beta-counter – 300 SL Automatic TDCR Liquid Scintillation Counter (HIDEX, Finland)- and a liquid scintillation cocktail – Ultima Gold (high flash point LSC cocktail, biodegradable) was used.

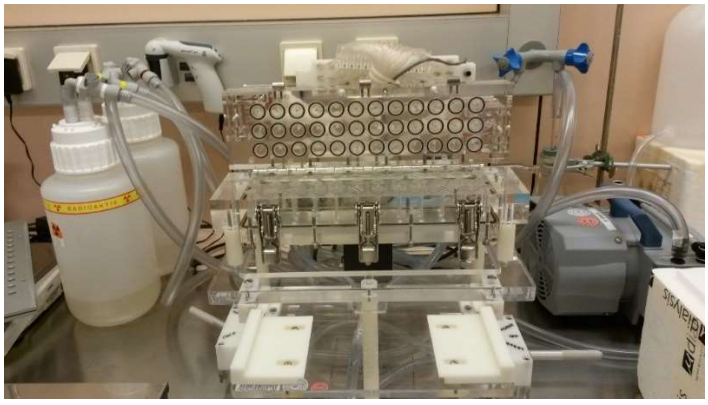

Figure 11: Brandel® Cell harvester, cell laboratory at medical university of vienna (Dep. Radiopharmacy)

Figure 12: Liquid scintillation beta-counter, HIDEX [28]

3.3 Methods

3.3.1 Preparation of assay buffer

Since the NET is sodium dependant, the buffer must contain amounts of sodium. [4,5]

All ingredients for the buffer should be well calculated, therefore the molecular weight had to be considered by the chemical structure of the compounds. The composition of the buffer was taken over from the autoradiography study from Gulyás et al. [7]

Substance	Concentration	Molecular weight	Weight portion
Potassium Chloride	5mM	74.55 g/mol	0.37275 g/l
Sodium Chloride	300mM	58.44 g/mol	17.532 g/l
TRIS	50mM	121.14 g/mol	6.057 g/l
Ascorbic Acid	0.1%	176.13 g/mol	0.176 g/l

Table 9: Assay buffer composition for NET

The chemicals mention above were completely dissolved in deionized water. Subsequently, the buffer was adjusted to pH 7.4 with HCl conc. To allow a defined binding protocol, the prepared buffer had to be cooled to 4°C, the ligands were dissolved at 0°C. [20]

3.3.2 Preparation of stock solutions of compounds

All compounds were prepared as a stock solution at concentration 5mM, shown in table 10.

After the precise mass was reported, the compound was solved in a composition of acetonitrile and distilled water in ratio 7:3. Focused on efficiently dissolution, a Vortex mixer was adapted for homogenous centrifugation.

Due to the lipophilicity of the test-compounds, the usage of acetonitrile as co-solvent was inevitably. Acetonitrile was aliquoted in all vials, so that the concentration was the same in the final volume.

Compound	Concentration	Molecular weight	Weight portion
FAPPI 1	5mM	375.45 g/mol	1.87725 g/l
FAPPI 2	5mM	375.45 g/mol	1.87725 g/l
FAPPI 3	5mM	375.45 g/mol	1.87725 g/l
PHOXI 1	5mM	283.37 g/mol	1.41685 g/l
Me@PHOXI 1	5mM	297.40 g/mol	1.487 g/l
Fe@PHOXI 1	5mM	329.42 g/mol	1.6471 g/l
PHOXI 2	5mM	337.34 g/mol	1.6867 g/l
Me@PHOXI 2	5mM	351.37 g/mol	1.75685 g/l
Fe@PHOXI 2	5mM	383.39 g/mol	1.91695 g/l
DIMAP	5mM	314.4 g/mol	1.572 g/l
Me@DIMAP	5mM	328.42 g/mol	1.6421 g/l
FE@DIMAP	5mM	360.44 g/mol	1.8022 g/l
MAPPI	5mM	294.39 g/mol	1.65425 g/l
Me@MAPPI	5mM	308.42 g/mol	1.5421 g/l
FE@MAPPI	5mM	340.43 g/mol	1.70215 g/l
HAPTHI	5mM	319.38 g/mol	1.66705 g/l
Me@HAPTHI	5mM	333.41 g/mol	1.73715 g/l
FE@HAPTHI	5mM	365.42 g/mol	1.89725 g/l
Reboxetine	5mM	313.40 g/mol	1.567 g/l
Nisoxetine	5mM	271.36 g/mol	1.3568 g/l

Table 10: Concentration of stock solutions

Further dilution of the stock solutions was done to achieve the following final concentration in the assays: 10µM, 1µM, 100nM, 30nM, 10nM, 3nM, 1nM and 0.1nM, respectively.

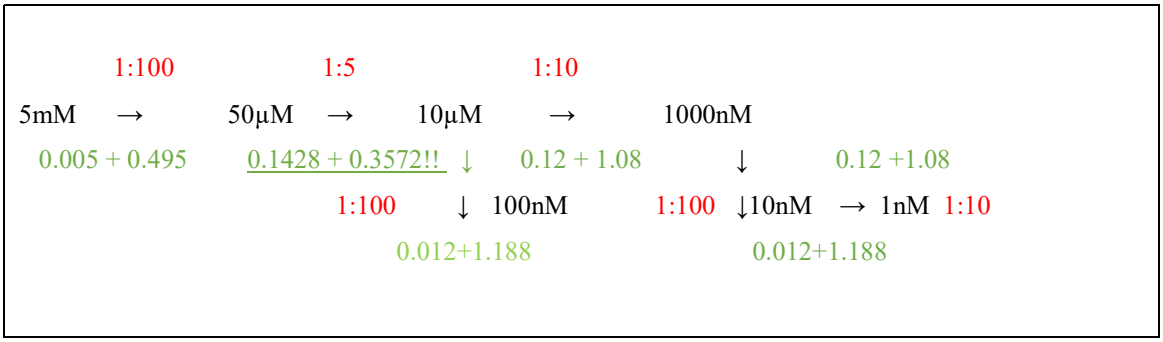

Table 11: Schema of dilution

3.3.3 Preparation of membranes

For the NET study the membrane target system was human NET (RHBNETM400UA).

The membranes with the size of 400 units were stored at -80°C. For the preparation of the study they needed to be separated into an equal amount of 8,0µl. In the following process of the work it was necessary to increase the quantity up to 16µl. For the aliquots the membrane was thawed to room temperature so that it could be pipetted very quickly in 1,5ml vials (Eppendorf®), positioned on ice, and immediately restored at -80°C.

Further utilization of the membranes had to be conducted on ice, shortly before the incubation of all compounds started, they were solved in assay buffer in a mixture of 1:500.

3.3.4 Preparation of Polyethylenimin 0.3%

Polyethylenimin (PEI 50% w/w) is a high-viscous solution at a concentration of 50% in deionised water. For the dilution of PEI 0.3% the amount of 60ml were taken out and resuspended with water.

The Waterman GF/C filter was pre-soaked in PEI 0.3% to reduce the unspecific binding.

3.3.5 Preparation of the radioligand

[^{3}H]-Nisoxetin as the radioligand for the NET study, solved in 0.25% ethanol and stored at -20°C, ought to be solved in assay buffer for the preferred concentration of 10µM. For that outcome it was required to dilute the radioligand for the level of 1:10000 in a quantity of 20ml.

The activity of the radioligand was 37MBq/ml with the specific activity of 3022.9GBq/mmol, accordingly to prepare the proposed dilution of 2nM.

3.3.6 Comparison of the conditions of NET, DAT, SERT

The conditions and comparability of the radioligand binding study are shown in the following table, including not only the settings for the studies on the NET but also for Dopamine transporter and the Serotonin transporter. The practice on the three membrane targets was performed for the assessment of the correlation of the difference between the transporters and selectivity of compounds.

Membrane target system	**hNET**	**hDAT**	**hSERT**
Protein concentration	3 µg/µL	12 µg/µL	9 µg/µL
Cellular background	MDCK	CHO-K1	HEK293
Radioligand	[^{3}H]-Nisoxetine	[^{3}H]-WIN 35,428	[^{3}H]-Imipramine
Radioligand concentration	4nM	25nM	2nM
Activity concentration	3119 GBq/mmol	3056 GBq/mmol	1909 GBq/mmol
Reference compound	reboxetine	GBR12909	clomipramine
Reference concentration	10 µM	10 µM	200 µM
PEI	0.3%	0.5%	0.5%
Total volume	500 µl	500µl	500µl
↳ membrane	100 µl	100 µl	100 µl
↳ radioligand	50 µl	50 µl	50 µl
↳test compound	350 µl	350 µl	350 µl

Table 12: Comparison of NET/DAT/SERT

Substance	Concentration	Molecular weight	Weight portion
Potassium Chloride	5mM	74.55 g/mol	0.37275 g/l
Sodium Chloride	300mM	58.44 g/mol	17.532 g/l
TRIS	50mM	121.14 g/mol	6.057 g/l
Ascorbic Acid	0.1%	176.13 g/mol	0.176 g/l

Table 13: Assay buffer composition for NET

Substance	Concentration	Molecular weight	Weight portion
Potassium Chloride	-	-	-
Sodium Chloride	100mM	58.44 g/mol	5.844 g/l
TRIS	50mM	121.14 g/mol	6.057 g/l
Ascorbic Acid	-	-	-

Table 14: Assay buffer composition for DAT

Substance	Concentration	Molecular weight	Weight portion
Potassium Chloride	5mM	74.55 g/mol	0.37275 g/l
Sodium Chloride	120mM	58.44 g/mol	7.0128 g/l
TRIS	50mM	121.14 g/mol	6.157 g/l
Ascorbic Acid	-	-	-

Table 15: Assay buffer composition for SERT

Substance	Concentration	Molecular weight	Weight portion
Potassium Chloride	-	-	-
Sodium Chloride	154mM	58.44 g/mol	8.9997 g/l
TRIS	50mM	121.14 g/mol	6.157 g/l
Ascorbic Acid	-	-	-

Table 16: Wash buffer composition for SERT

4 Instrumentation

For the M-36 tygon tubed Cell harvester (Brandel®, Gaithersburg, USA) 36 glass vials were used with 500µl total volume, containing 350µl standard compound, 50µl radioligand and 100µl membrane suspension, following a standard protocol shown in tab.17.

No.	Substance	Conc.	Radioligand 3H-Nisoxetin	Membrane suspension	Standard of Substance
1-3	control	buffer	50µl	100µl	350µl
4-6	HAPTHI	1000nM	50µl	100µl	350µl
7-9		100nM	50µl	100µl	350µl
10-12		10nM	50µl	100µl	350µl
13-15	Me@HAPTHI	1000nM	50µl	100µl	350µl
16-18		100nM	50µl	100µl	350µl
19-21		10nM	50µl	100µl	350µl
22-24	FE@HAPTHI	1000nM	50µl	100µl	350µl
25-27		100nM	50µl	100µl	350µl
28-30		10nM	50µl	100µl	350µl
31-33		1nM	50µl	100µl	350µl
34-36	Reboxetine	10µM	50µl	100µl	350µl

Table 17: Schema of pipetting, numbers represent position in the rack

Normally the control and reference were placed in rack-numbers at the front and at the back, in addition three compounds in decreasing concentrations could be tested in one assay.

Before starting the experiment, some basic steps needed to be done:

- the glass tubes had to be dry and without scratches or other damages
- all compounds, references, radioligand, membrane, buffer and PEI composed in their right concentration and solvent

Procedure of competitive binding application:

1. Addition of the compounds following the order shown in the table, starting with the standards using a pipette (Eppendorf Reference)
2. Addition of the radioligand, using the multipette® 4780 (Eppendorf Original Model 4780 Repeating pipette)
3. Addition of the homogenous thawed membrane suspension, using the multipette® 4780 (Eppendorf Original Model 4780 Repeating pipette)
4. Incubation time for 1h shaking on a water bath at room temperature to achieve equilibration of binding
5. Pre-soaking of the filter (GF/C) in 0.3%-PEI for 10min
6. Filter positioning on the filtration plate and closing
7. After the incubation the samples were filtered on the cell harvester with ice-cold wash buffer
8. Two times filtering hot (radioactive wash-water needed to be collected in the hot trash bottle for special decontamination)
9. Two times filtering cold
10. After filtering: transfer of filter in a special squeezing device (a) and push through with special device (b) to achieve filter parts for the counting
11. Incubation of the filter parts in the pico hang-in vials for 30min - soaking with 2ml scintillation cocktail
12. Measurement of radioactivity in the beta-counter

Figure 13: Multipette® 4780 / repeater pipette 4780

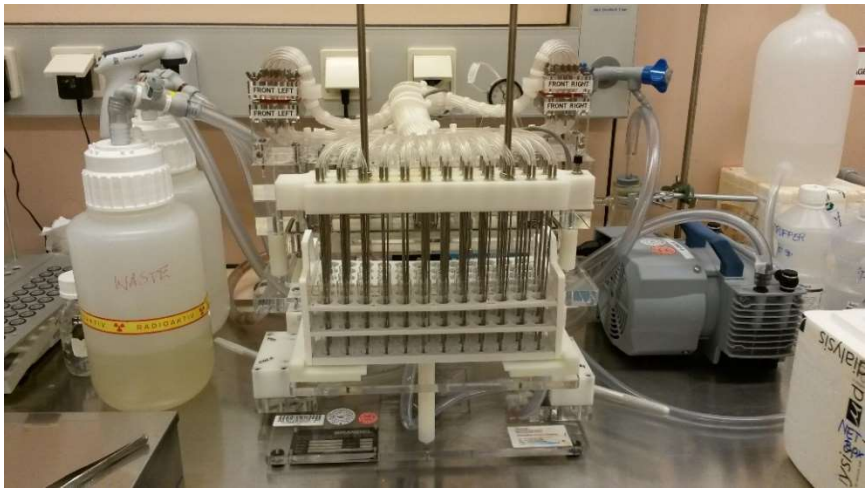

Figure 14: Brandel® Cell harvester

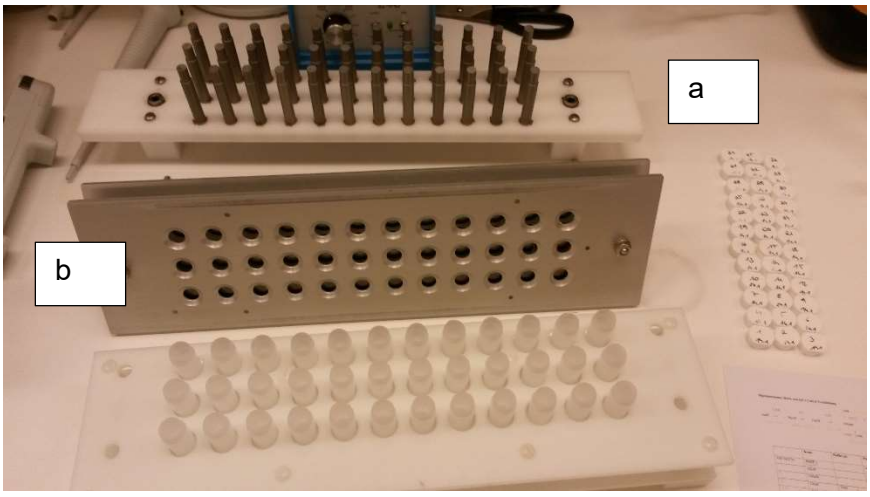

Figure 15: Special device, a: squeezing plate, b: push through system

4.1.1 Counting of radioactivity

The final steps of the binding assay were the counting of the radioactivity of the tritiated probes. On that account, the liquid scintillation counting is assumed as the gold standard method.

Considering the weak radioactivity of tritium – "*the mean energy of beta emission from ^{3}H is only about 5.5kev"* [25], the effect of efficiency needed to be concerned for the total activity, so the tritium standards were utilized to attempt the calculation for the efficiency-standard for 5ml and 15ml volumes. Therefore, the counts per minute were in ratio to the disintegrations per minute.

$$\% E = \frac{CPM}{DPM} * 100$$

Efficiency percentage equation [26,27]

Volume of one vial	efficiency
5ml	67.83%
15ml	66.93%

Table 18: Efficiency

This efficiency was applied for the equation of the real and actual concentration of the radioligand due to the calculation of specific activity was needed. Hence, the specific radioactivity was transmuted from Ci/mmol into cpm/fmol, known as counts per minute.

Y cpm/fmol = X Ci/mmol * 2.2*E

For the calculation of the K_i levels, the concentration of the radioligand had to be transformed into the actual concentration with following equation:

$$\frac{\frac{cpm}{E} * \frac{100}{1110}}{specific\ acitivity} = RL\ (nM)$$

$$\frac{\frac{118294.26}{67.83} * \frac{100}{1110}}{82} = 1.91\ (nM)$$

The equation for the K_i was performed by the Cheng and Prusoff formula: [19]

$$Ki = \frac{\text{IC50}}{1 + \frac{[radioligand]}{\text{Kd}}}$$

$$Ki = \frac{0.95}{1 + \frac{[1.91]}{0.8}} = 0.28\ nM$$

5 Analysis

For the analysis of data, the GraphPad Prism Software, which is a software program for simplifying common equations and curve fittings in science data organization, was utilized. The probes of the study were triplicates, their radioactivity of the bound radioligand was measured in the beta counter, where the CPM-data was obtained (fig). The following figures display the table of files on the computer, saved as screenshots to clarify the steps of the operation.

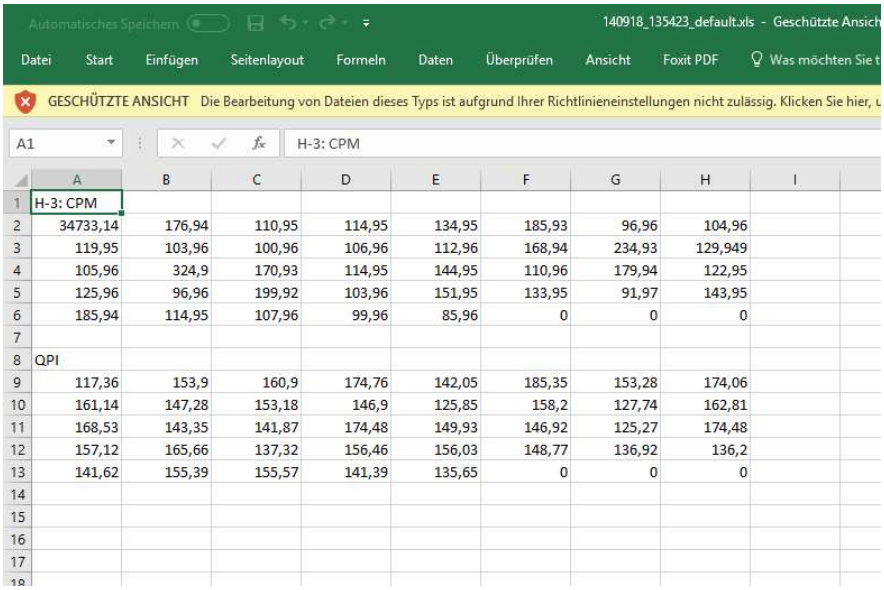

	A	B	C	D	E	F	G	H	I
1	H-3: CPM								
2	34733,14	176,94	110,95	114,95	134,95	185,93	96,96	104,96	
3	119,95	103,96	100,96	106,96	112,96	168,94	234,93	129,949	
4	105,96	324,9	170,93	114,95	144,95	110,96	179,94	122,95	
5	125,96	96,96	199,92	103,96	151,95	133,95	91,97	143,95	
6	185,94	114,95	107,96	99,96	85,96	0	0	0	
7									
8	QPI								
9	117,36	153,9	160,9	174,76	142,05	185,35	153,28	174,06	
10	161,14	147,28	153,18	146,9	125,85	158,2	127,74	162,81	
11	168,53	143,35	141,87	174,48	149,93	146,92	125,27	174,48	
12	157,12	165,66	137,32	156,46	156,03	148,77	136,92	136,2	
13	141,62	155,39	155,57	141,39	135,65	0	0	0	
14									
15									
16									
17									

Figure 16: CPM data values

This CPM-excel-file was transferred into GraphPad analysis-software and plotted against the concentrations of the compounds.

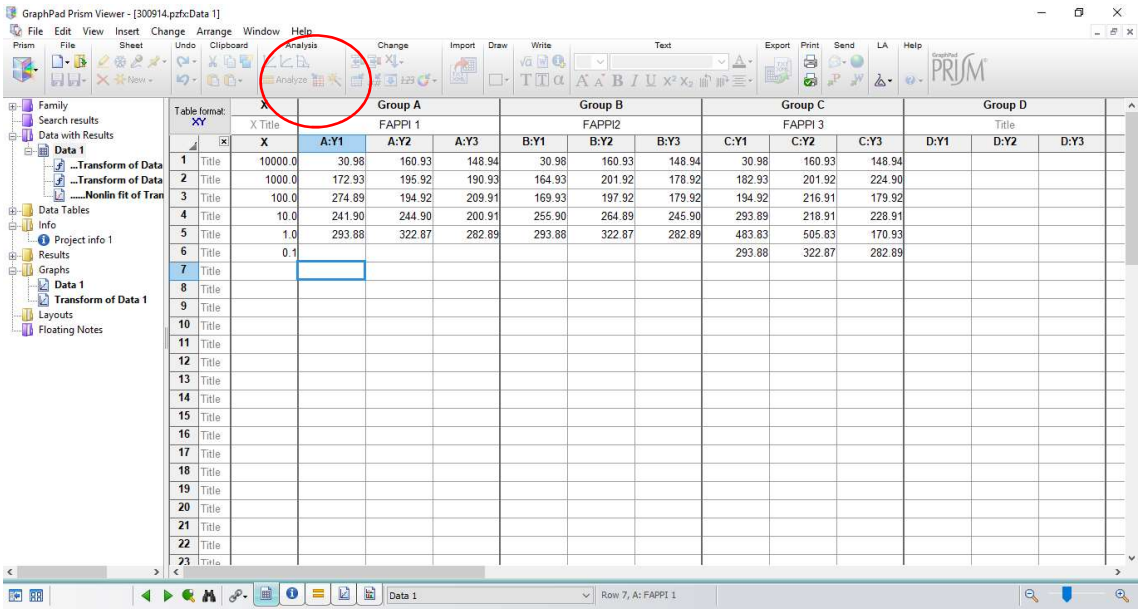

Figure 17: First analysing step of transformation of cpm-data

The elements of the software were *"analyze"* and its function *"transform of"* to reach the comparison of *"X=log(X)"*.

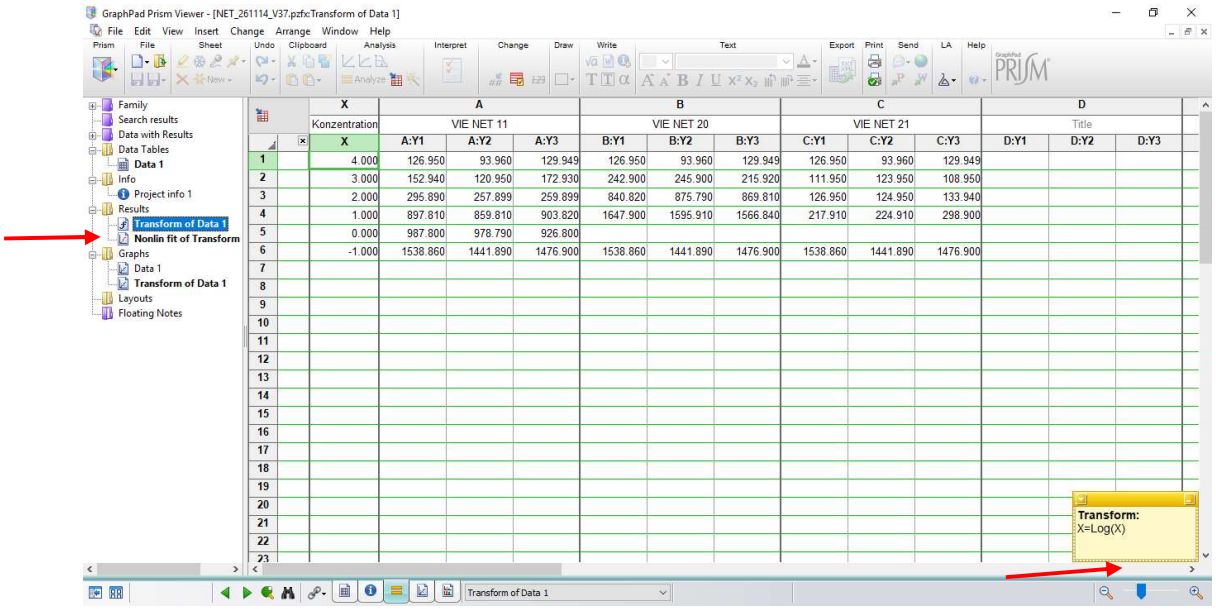

Figure 18: Measured data plotted against log concentration

After transformation of data, the nonlinear fit of data, representing *"log(inhibitor) vs. response (three parameters)"*, was obtained.

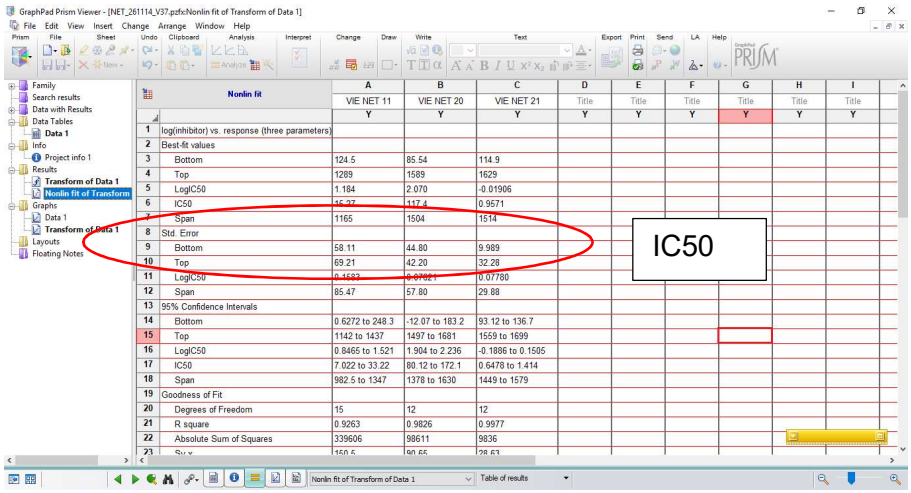

Figure 19: File with resulted terms

The evaluation of the K_i levels was attained by the equation of Cheng and Prusoff including the values of $IC_{50,}$ received from the GraphPad software.

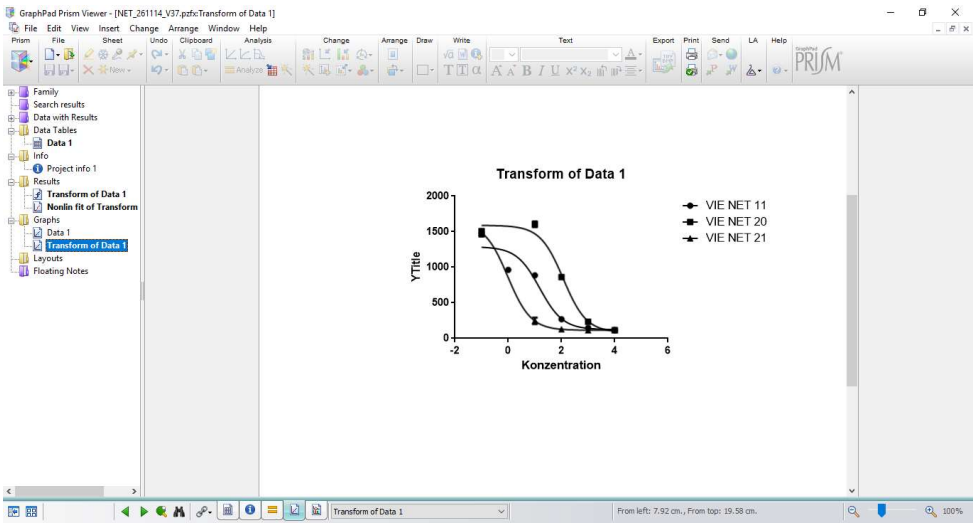

Figure 20: Dose-response curve: competitive binding of tested compounds

The applied curves of the competition tests represent the function of *"log(inhibitor) vs response-variable slope".*

As a memento of evidence of the curve: the competitive binding curve demonstrates the affinity to the receptor of the examined compounds after the competition of the binding to the receptor among the radioligand and antagonist. In detail, the IC50 explains the half value when the binding of the radioligand is blocked by the unlabelled testing compound.

6 Results

The received results of the binding studies evince a comparison of a score of new compounds with expectantly affinity to NET, as well to DAT and SERT.

The hereinafter evaluation of results is separated into the different chemical structure of the tested compounds. A summary of all tested compounds follows the isolated results.

All evaluated samples are triplicates in each trial, chiefly combined in their similar chemical structure (as far as available).

6.1 Results of compounds at NET

6.1.1 Results of FAPPIs – benzo[d]imidazolone derivatives

Compound	**FAPPI 1**	**FAPPI 2**	**FAPPI 3**
Ki (nM)	5.317681301	28.88985025	72.92178999
	6.16142538	37.5962724	20.661295
	8.41656733	19.1955762	21.4730372
	10.3746855	69.4398783	8.00470483
	15.6699359	199.376825	11.9278194
	23.8513958	24.311643	28.4707717
	9.29504937	33.8220362	9.43843942
	7.94925564	22.4277926	25.3126704
	8.98840747	38.74810374	13.2612412
	6.886392935	151.321501	17.56432668
	6.32432596	20.02696325	34.7334115
	2.976435022	31.1450151	16.37712664
	8409423266	20.34050053	33.21776027
	6.520421115		21.04475957
	13.7766271		72.5024436
MV	**9.39453527**	**49.7601398**	**27.1274398**
STD	4.932738749	54.08130017	19.45205821
Hill slope	-0.1064	-0.02009	-0.0343
Number of trials	15	13	15

Table 19: Results of FAPPI

The table 18 shows the affinity of FAPPI 1, FAPPI 2 and FAPPI 3 as mean values.

FAPPI 1 demonstrates a Ki value of 9.39nM ± 4.93; this displays a higher affinity to NET than its derivatives FAPPI 2 (Ki 49.76nM ± 54.08) and FAPPI 3 (Ki 27.13nM ± 19.45), although the competition curve (see figure 21) is very similar. The ratio of FAPPI 2/FAPPI 1 is 2.815 and FAPPI 3/FAPPI 1 is 1.323; this concludes to a higher selectivity to NET.

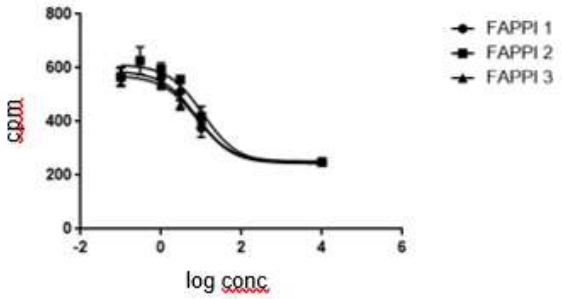

Figure 21: Competitive binding curve of FAPPI 1, FAPPI 2, FAPPI 3

The curve shows significant affinity of all three FAPPI derivatives to NET.

6.1.2 Results of PHOXIs – phenoxyisochromen derivatives

Compound	**PHOXI 1**	**Me@PHOXI 1**	**Fe@PHOXI 1**
Ki (nM)	2.70050266	436.061735	1685.78215
	2.30749069	50.80917	854.769989
	5.83269427	139.141722	1347.29015
MV	**3.61356254**	**208.670876**	**1295.94743**
STD	1.57734457	164.783923	341.196288
Hill slope	-0.276	-0.0060	-0.00077
Number of trials	3	3	3

Table 20: Results of PHOXI 1

The higher affinity of PHOXI 1 is evident by the Ki value of 3.61nM ± 1.57 in contrast to Me@PHOXI 1 (Ki = 208.67nM ± 164.7) and Fe@PHOXI 1 (Ki = 1295.9nM ± 341.19). Calculated ratio for Me@PHOXI 1/ PHOXI 1 is 57.80 and 358.98 for Fe@PHOXI1/PHOXI 1.

	PHOXI 2	Me@PHOXI 2	Fe@PHOXI 2	Me@PHOXI 3
Ki (nM)	0.9966284	21.5289639	453.555441	32.8125339
	0.95999357	327.52722	436.99255	29.2101366
	0.47066475	434.070003	494.029089	36.1077501
MV	**0.80909558**	**261.042062**	**461.525694**	**32.7101402**
STD	0.23977364	174.857531	23.9573981	2.81686959
Hill slope	-1.235	-0.00383	-0.00216	-0.03057
Number of trials	3	3	3	3

Table 21: Results of PHOXI 2

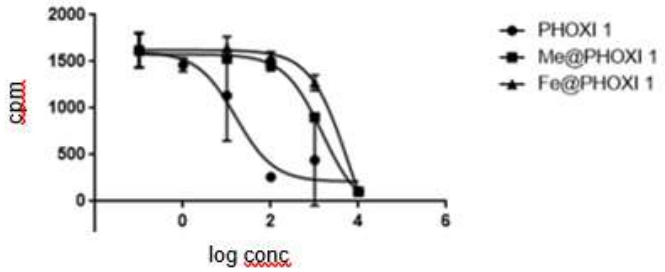

Figure 22: Competitive binding curve of PHOXI 1, Me@PHOXI 1, FE@PHOXI 1

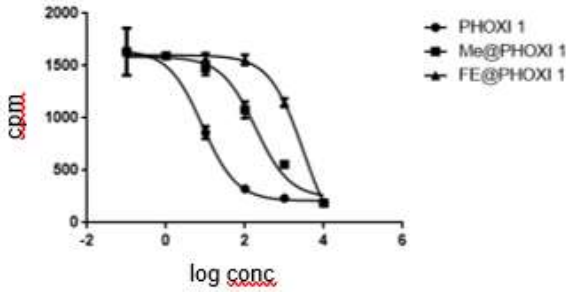

Figure 23: Competitive binding curve of PHOXI 1, Me@PHOXI 1, FE@PHOXI

The two curves present the evaluation with (fig.22) and without (fig.23) one-off data. Obviously, there is no significant difference for PHOXI 1 except of the decreasing span, but Me@PHOXI 1 is showing a switch to the left, interpreted as better competition to the reference than the variations due to the higher steepness of the curve.

The effects of the variations of PHOXI 2 describe high affinity of PHOXI 2 at Ki 0.80nM ± 0.23, whereas Me@PHOXI 2 (Ki = 261.04 nM ± 174.85) and FE@PHOXI

2 (Ki = 461.52nM ± 23.95) are not affine; so, the ratio is 322.66 for Me@PHOXI 2/ PHOXI 2 and 570.48 for FE@PHOXI 2/ PHOXI 2 and manifests higher selectivity for PHOXI 2.

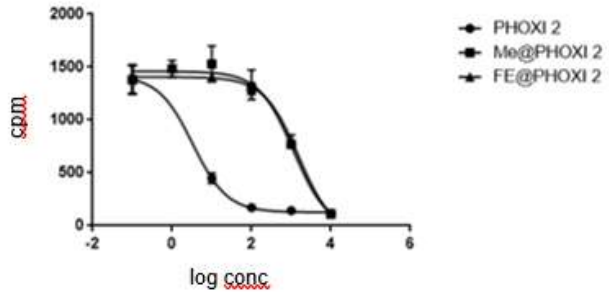

Figure 24: Competitive binding curve of PHOXI 2, Me@PHOXI 2, FE@PHOXI 2

Figure 24 pictures the representative competitive binding curve with higher affinity of Me@PHOXI 2.

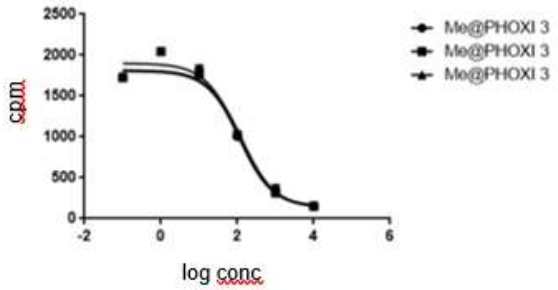

Figure 25: Competitive binding curve of Me@PHOXI 3

The data of PHOXI 3 are not entirely examined due to the set of compounds was not available at the time of the study. Hence, the Ki value for Me@PHOXI 3 is 32.71nM ± 2.81) and displays moderate affinity to NET.

6.1.3 Results of DIMAPs – indolinyl derivatives

Compound	DIMAP	Me@DIMAP	FE@DIMAP
Ki (nM)	101.007832	3.23970637	1782.57816
	72.3902934	3.56286658	1244.7672
	43.9004852	8.31241907	896.661146
	83.6006325	5.31741592	6121.09051
	98.175225	4.01121609	3186.2142
		4.49772132	
		3.953740058	
		1.861010651	
		3.05043899	
		2.07021254	
		3.833390941	
		4.77588952	
		2.68820138	
MV	**79.8148935**	**3.93647919**	**2646.26224**
STD	20.71493968	1.589649539	1904.585108
Hill slope	-0.0125	-0.2540	-0.00037
Number of trials	5	13	5

Table 22: Results of DIMAP

The methylated compound Me@DIMAP (Ki 3.93nM ± 1.58) expresses higher affinity to NET than the precursor DIMAP (Ki 79.81nM ± 20.71) and the fluorethylated FE@DIMAP (Ki 2946.26nM ± 1904.58). Better selectivity of Me@DIMAP is certified as ratio: DIMAP/ Me@DIMAP 20.30 and FE@DIMAP/ Me@DIMAP 673.34.

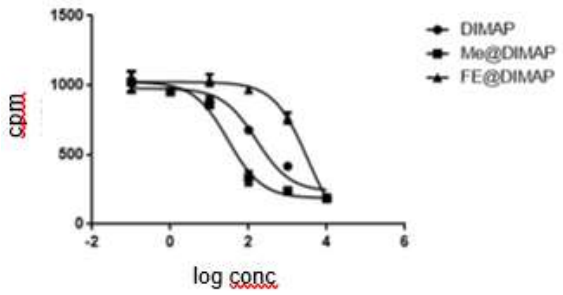

Figure 26: Competitive binding curve of DIMAP, Me@DIMAP, FE@DIMAP

Leading affinity of Me@DIMAP is visible as first curve in figure 26.

The illustration in figure 27 shows Me@DIMAP (VIENET 11), combined with HAPTHI (VIENET 20) and Me@HAPTHI (VIENET 21).

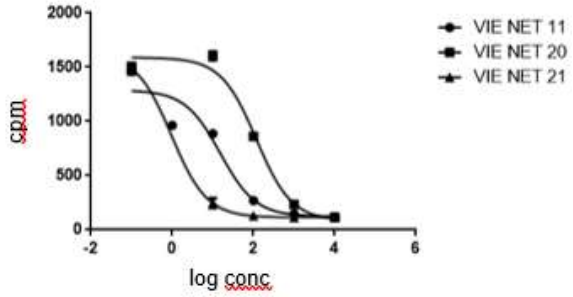

Figure 27: Competitive binding curve of DIMAP, Me@DIMAP, FE@DIMAP

6.1.4 Results of MAPPIs – indolinole derivatives

Compound	MAPPI	Me@MAPPI	FE@MAPPI
Ki (nM)	1047.434725	45.96415096	37552.16841
	1949.153294	89.32739366	26810.35211
	1091.06926	60.8792252	999.479383
	1257.741587	492.807008	2135.60977
	1730.04505	80.0510381	57584.0653
	1094.46217	62.6553625	42.1557571
	1281.86707	65.8172659	232.5508931
	4916.3034	22.1493599	124681.2248
	2079.79478	286.0266291	61421.76709
	97.05950481	74124.13317	206.8492384
	78048.93516	89.93543859	40853.8743
	35.3835413	59.23608263	85.31867414
	118417.5332	36.48763849	65638.06515
	49.23559738	9799.02642	77585.515
	13894.57174	32697.52133	79226.16431
	8558.47607	28.3460551	5531.785287
	8739.456481	28.94547029	
	3365.55093	67.1606805	
	3374.71162	67.343485	
	1501.44359	58.30180344	
	1105.66371	76.1262679	
	1474.67112	64.2721044	
MV	**1796.00957**	**114.956351**	**20853.9718**
STD	1217.968941	144.0892879	21760.50566
Hill slope	-0.000556	-0.00869	-0.000047
Number of trials	22	22	16

Table 23: Results of MAPPI

The overabundance of experiments of the derivatives of MAPPI is based on the process of elimination of systematic error due to the exorbitant high values of Ki.

Since there is no valid affinity to NET, the Ki values are: 1796.00nM ± 1217.96 for MAPPI, 114.95nM ± 144.089 for Me@MAPPI and 20853.97nM ± 21760.50 for FE@MAPPI. The ratio for MAPPI towards Me@MAPPI counts 15.62 and for FE@MAPPI towards Me@MAPPI is 181.4, so that Me@MAPPI is more selective to NET than the others.

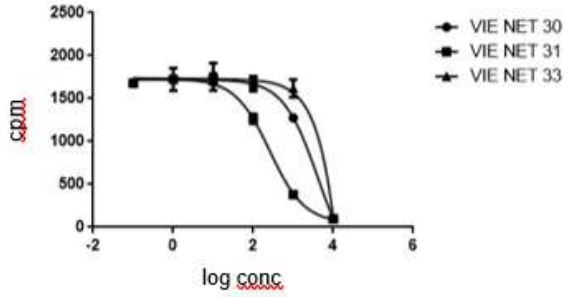

Figure 28: Competitive binding curve of MAPPI, Me@MAPPI, FE@MAPPI

In figure 28: Me@MAPPI conveys more affinity to NET towards MAPPI and FE@MAPPI.

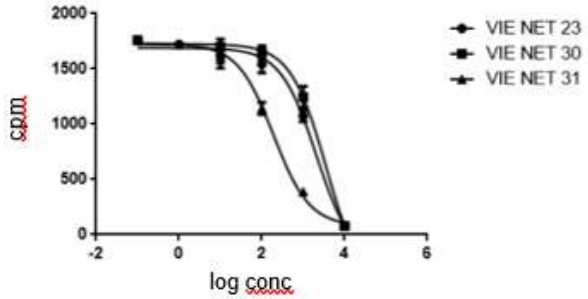

Figure 29: Competitive binding curve of FE@HAPTHI, MAPPI, FE@MAPPI

Me@MAPPI (VIENET 31) in contrast to FE@HAPTHI (VIENET 23) and MAPPI (ViENET 30) reveals more affinity.

6.1.5 Results of HAPTHIs – thiadiazole derivatives

Compound	HAPTHI	Me@HAPTHI	FE@HAPTHI
Ki (nM)	34.5797304	0.28191022	714.7273276
	37.69845171	0.269549676	187.403502
	1.885637651	0.186648332	678.5058202
	21.2025433	0.06689715	376.6170857
	18.3947948	0.1894333	535.411043
	19.47956237	0.19245896	626.175895
	34.2709791	0.2670348	106605.107
	26.0065356	0.18919459	38.3676917
MV	**24.1897794**	**0.20539088**	**13720.2894**
STD	10.94036568	0.065180068	35107.88102
Hill slope	-0.04133	-4.8687	-0.0000728
Number of trials	8	8	8

Table 24: Results of HAPTHI

Table 23 represents the most suitable results in behaviour of novel tracers on NET. The Ki values are: HAPTHI 24.18nM ± 10.94, Me@HAPTHI 0.205nM ± 0.065, FE@HAPTHI 13720.28nM ± 35107.88. For validation the ratios of Me@HAPTHI are: HAPTHI/Me@HAPTHI 117.95 and FE@HAPTHI/Me@HAPTHI 66928.19; this is a certification for Me@HAPTHI: it shows the highest affinity and selectivity to NET in contrast to the other compounds of the variations of HAPTHI.

In addition to that, the competitive binding curve (fig. 30) conducts to the same conclusion. Namely, compared to Me@DIMAP (VIENET 11) and HAPTHI (VIENET 20), Me@HAPTHI (VIENET 21) displays a significant curve in the competition.

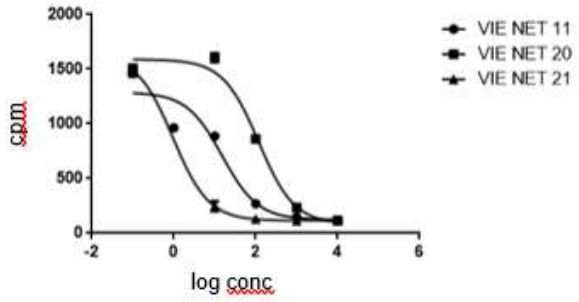

Figure 30: Competitive binding curve of Me@DIMAP, HAPTHI, Me@HAPTHI

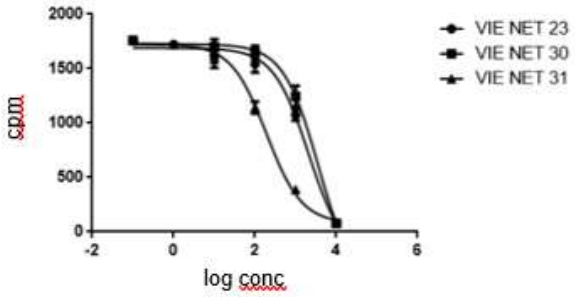

Figure 31: Competitive binding curve of FE@DIMAP, MAPPI, Me@MAPPI

Figure 31 demonstrates the higher affinity of FE@HAPTHI (VIENET 23) in divergence to MAPPI (VIENET 30) and Me@MAPPI (VIENET 31).

6.1.6 Final results NET

Compound	Ki (nM)
FAPPI 1	9.39 ± 4.93
FAPPI 2	49.76 ± 54.08
FAPPI 3	27.12 ± 19.45
PHOXI 1	3.613 ± 1.5
Me@PHOXI 1	208.67 ± 164.78
Fe@PHOXI 1	1295.94 ± 341.19
PHOXI 2	0.80 ± 0.23
Me@PHOXI 2	261.04 ± 174.85
Fe@PHOXI 2	461.52 ± 23.95
Fe@PHOXI 3	32.71 ± 2.81
DIMAP	79.81 ± 20.71
Me@DIMAP	3.93 ± 1.58
FE@DIMAP	2646.26 ± 1904.58
MAPPI	1796.00 ± 1217.96
Me@MAPPI	114.95 ± 144.08
FE@MAPPI	20853.97 ± 21760.50
HAPTHI	24.18 ± 10.94
Me@HAPTHI	0.20 ± 0.06
FE@HAPTHI	13720.28 ± 35107.88

Table 25: Affinity at NET

To conclude the results of the compounds at NET, five of them express high affinity:

- FAPPI 1 Ki 9.39nM ± 4.93
- PHOXI 1 Ki 3.61nM ± 1.5
- PHOXI 2 Ki 0.8nM ± 0.23
- Me@DIMAP Ki 3.93nM ± 1.58
- MeHAPTHI Ki 0.2nM ± 0.06

6.2 Results DAT

Compound	Ki (nM) MV	STD	n
FAPPI 1	6558797.8	9245701.72	3
FAPPI 2	7373414.54	10299496.5	3
FAPPI 3	35962057	37477641.9	3
DIMAP	28366650.5	28357431.84	2
Me@DIMAP	10712960.8	10681315.61	2
FE@DIMAP	10217145.6	10156863.33	2
MAPPI	35113304.4	35100607.1	2
Me@MAPPI	10622234.7	10456116.2	2
FE@MAPPI	111903968	91367905.2	2
HAPTHI	1071.786504	504.0789042	3
Me@HAPTHI	1655.144753	669.5818703	3
FE@HAPTHI	1744.242123	1025.898234	3

Table 26: Affinity at DAT

The related outcomes of all tested compounds proclaim no affinity to DAT. The results (tab.17) reveal Ki values ≥1000nM up to ≥10µM.

6.3 Results SERT

Compound	Ki (nM) MV	STD	n
FAPPI 1	88.4631408	14.4967341	2
FAPPI 2	529.283267	83.9194251	2
FAPPI 3	180.433799	11.237201	2
DIMAP	1625.08489	528.967841	4
Me@DIMAP	1942.58805	1830.441	4
FE@DIMAP	13586.3704	2794.35983	4
MAPPI	2001.82502	1705.20763	4
Me@MAPPI	5371.75914	2957.5690	4
FE@MAPPI	31895.3851	4765.84221	4
HAPTHI	8070.221225	8013.971588	4
Me@HAPTHI	652.8195984	43.06864644	4
FE@HAPTHI	15682.57082	27138.83498	4

Table 27: Affinity at SERT

Pictured in table 18, the samples demonstrate equally no affinity to SERT. Ki levels ≥1500nM for the “DIMAP-group”, Ki ≥2000nM for MAPPI’s and ≥650nM for HAPTHI’s attest neither affinity nor selectivity to SERT. Even the values of FAPPI can be neglected (FAPPI 2 Ki 529.28nM ± 83.9 and FAPPI 3 Ki 180.43 ± 11.23), although the Ki is 88.46nM ± 14.49 for FAPPI 1.

6.4 Results: a comparison of NET:DAT:SERT

Compound	NET	DAT	SERT
	Ki (nM) MV	Ki (nM) MV	Ki (nM) MV
FAPPI 1	9.39 ± 4.93	6558797.8 ± 9245701.72	88.46314 ± 14.496
FAPPI 2	49.76 ± 54.08	7373414.54 ± 10299496.5	529.2832 ± 83.919
FAPPI 3	27.12 ± 19.45	35962057 ± 37477641.9	180.4337 ± 11.23
PHOXI 1	3.613 ± 1.5	n.v.	n.v.
Me@PHOXI 1	208.67 ± 164.78	n.v.	n.v.
Fe@PHOXI 1	1295.94 ± 341.19	n.v.	n.v.
PHOXI 2	0.80 ± 0.23	n.v.	n.v.
Me@PHOXI 2	261.04 ± 174.85	n.v.	n.v.
Fe@PHOXI 2	461.52 ± 23.95	n.v.	n.v.
Fe@PHOXI 3	32.71 ± 2.81	n.v.	n.v.
DIMAP	79.81 ± 20.71	28366650.5 ± 28357431.8	1625.084 ± 528.96
Me@DIMAP	3.93 ± 1.58	10712960.8 ± 10681315.61	1942.588 ± 1830.4
FE@DIMAP	2646.26 ± 1904.58	10217145.6 ± 10156863.33	13586.37 ± 2794.3
MAPPI	1796.00 ± 1217.96	35113304.4 ± 35100607.1	2001.825 ± 1705.2
Me@MAPPI	114.95 ± 144.08	10622234.7 ± 10456116.2	5371.759 ± 2957.5
FE@MAPPI	20853.97 ± 21760.50	111903968 ± 91367905.2	31895.38 ± 4765.8
HAPTHI	24.18 ± 10.94	1071.78650 ± 504.078904	8070.221 ± 8013.9
Me@HAPTHI	0.20 ± 0.06	1655.14475 ± 669.5818703	652.8195 ± 43.068
FE@HAPTHI	13720.28 ± 35107.88	1744.24212 ± 1025.8982	15682.57 ± 27138.83

Table 28: Affinity of compounds at NET, DAT, SERT

Compound	DAT/NET ratio	SERT/NET ratio
FAPPI 1	698487.519	9.42099476
FAPPI 2	148179.553	10.6367216
FAPPI 3	1326034.55	6.65316368
DIMAP	355427.271	20.3619207
Me@DIMAP	2725944.22	494.297214
FE@DIMAP	3860.97572	5.1341782
MAPPI	19550.8376	1.1146019
Me@MAPPI	92407.4354	46.731267
FE@MAPPI	5366.07504	1.52946346
HAPTHI	44.325331	333.756047
Me@HAPTHI	8275.72377	3264.09799
FE@HAPTHI	0.12712876	1.14302119

Table 29: Selectivity of compounds

Compound	DAT/NET ratio	SERT/NET ratio
FAPPI 1	698487	9.4
Me@DIMAP	2725944	494
Me@HAPTHI	8275	3264

Table 30: Higher affinity of selective compounds at NET

In table 30, a comparison of the compounds with higher affinity at NET is demonstrated. FAPPI 1 shows ≥500000 times more affinity at NET than at DAT and 9 times more than at SERT. Me@DIMAP is ≥2000000 times selective at NET than at DAT and 494 times more than at SERT. Me@HAPTHI appears ≥8000 times worse selective at DAT and ≥3000 times worse at SERT than its affinity at NET.

The influence of diverse factors may be an outlook for optimisation of the assay-conditions. The first contributing coefficient, was the determination of initial suitable values by utilizing glass tubes. The previous use of plastic tubes did not display valid effects. Accordingly, the latency time for the appropriate vials for the beta

counter complicated the step of the transfer from filter into vials. In addition to this problem, former vials, which did not fit into the squeezing plate, were used until trial number 10; regarding that, a rack for optimization the transfer of the filter was assembled (a paper-folded box for the vials, which needed to be compressed by rubber bands). Thus, the transfer of the filter proclaimed another limiting factor of this work; namely, the soaked filter could rupture while transferring on the plate, so this was a carefully done step. Accordingly, the calculation of FAPPI1:3 neglected the outcomes of trial 1:10.

Incubation time and temperature conduct important coefficients to this assay; hence, the composition of the assay buffer was dominating the effects on the membranes, especially the sodium concentration. The temperature of the buffer for the filtration revealed as contribution for optimal quenching to reduce non-specific binding.

7 Discussion

The focus of this study was to acquire values of new potent PET tracers in regard of their affinity and selectivity to the NET. From this perspective, the compounds were obtained from ABX advanced biochemical compounds, Biomedizinische Forschungsreagenzien GmbH Radeberg, Germany and university of Vienna (department of pharmaceutical chemistry-division of drug synthesis) to investigate a screening towards their pharmacological profile.

The aim was to demonstrate the affinity of the diverse types of structures - not based on reboxetine, which represents the leading antagonist of NET. Therefore, these chemical structure types were examined in vitro: benzo[d]imidazolone derivatives (FAPPI); phenoxyisochromen derivatives (PHOXI); indolinyl derivatives (DIMAP); indolinole derivatives (MAPPI) and thiadiazole derivatives (HAPTHI).

Among the deposit of promising compounds, five are raising high affinity (≤10nM) and selectivity to NET: FAPPI 1 (9.39nM ± 4.93), PHOXI 1 (3.61nM ± 1.5), PHOXI 2 (0.80nM ± 0.23), Me@DIMAP (3.93nM ± 1.58), Me@HAPTHI (0.20nM ± 0.06).

Generally spoken, the methylated compounds showed the highest affinity to NET, followed by the unmethylated precursor and the lowest affinity was shown by the fluorehylated compounds.

FAPPI 1 is a fluorinated methyl amine, which demonstrated similar binding at the NET in docking studies like the reference compound Me@APPI. [38] The different position for fluorination displays a certain role for the successful binding (chemical structure shown in tab.1).

PHOXI 1 and PHOXI 2, both precursor for their methylated and fluormethylated variation, express high affinity at the NET, although their chemical structure – phenoxyisochromen - differs from all others (shown in tab. 2 and tab. 3).

The methylated version of DIMAP has almost identical values like PHOXI 1, nevertheless they are not chemical comparable.

Me@HAPTHI revealed the most prominently Ki values, 0,20nM ± 0,06; the reproduceable results offer a widely range in further investigations. Also selectivity to NET compared to DAT and SERT showed promising effects.

Therefore - Me@HAPTHI being the best candidate PET ligand – was started to be set up as ^{11}C-radiolabelled PET-ligand for the first time. The radiosynthesis and preclinical evaluation (in vitro test, logD analysis, autoradiography) confirm [^{11}C]Me@HAPTHI as a potent novel PET-tracer to ease clinical NET imaging. The outcomes of this in vitro testing in human brain tissues manifested Me@HAPTHI as promising novel NET PET-tracer: high uptake in NET-rich regions, proved by immunohistochemistry; suitable metabolic stability (30% intact tracer for ≥60min); radiosynthesis of sterile, formulated [^{11}C]Me@HAPTHI was performed within 39min and 5min quality control.[39]

In order to that, new implications of [^{11}C]Me@HAPTHI demonstrate the use in visualisation and assessment of sympathetic denervation post-myocardial infarction in rats. This preclinical in vivo evaluation is an enhancement of the thiadiazole derivate to allow accurate estimation of cardiac neuronal function. [40]

These observations enhance the progress in supplementary research at the norepinephrine transporter.

8 Conclusion

In conclusion, this investigation illustrated five appropriate novel ligands for the PET-imaging at the norepinephrine transporter. They combine low Ki values, emphasizing leading affinity and selectivity towards NET.

These arrangements certify the opportunity of an application of Me@HAPTHI as routine NET PET-tracer. The on-going research of Me@HAPTHI may improve the suitability of this compound for the clinical diagnosis.

9 References

[1] Zhou J. Norepinephrine transporter inhibitors and their therapeutic potential. Drugs Future. 2004; 29:1235-44

[2] Aktories K., Förstermann U., Hofmann F.B., Starke K. Allgemeine und spezielle Pharmakologie und Toxikologie. 2009; 10. Auflage, München, Elsevier Urban&Fischer

[3] Galli A., De Felice L.J., Duke B.J., Moore K.R., Blakely R.D. Sodium-dependent norepinephrine-induced currents in norepinephrine-transporter-transfected HEK-293 cells blocked by cocaine and antidepressants. The Journal of Experimental Biology. 1995; 198:2197–2212

[4] Kristensen A.S., Andersen J., Jørgensen T.N., Sørensen L., Eriksen J., Loland C.J., Strømgaard K., Gether U. SLC6 Neurotransmitter Transporters: Structure, Function and Regulation. Pharmacol Rev. 2011; 63:585-640

[5] Torres G.E., Gainetdinov R.R., Caron M.G. Plasma membrane monoamine transporters: structure, regulation and function. Nat Rev Neurosci. 2003; 4(1):13-25

[6] Rang H.P., Dale M.M., Ritter J.M., Flower R.J., Henderson G. Rang and Dale's Pharmacology. 2012; 7th edition, Elsevier Inc.

[7] Finch A. M., Sarramegna V. Graham R.M. Ligand Binding, Activation, and Agonist Trafficking. In: Perez D.M. (eds) The Adrenergic Receptors. The Receptors. Humana Press. 2006

[8] Tejani-Butt S.M. [3H] Nisoxetine: A radioligand for quantitation of norepinephrine uptake sites by autoradiography or by homogenate binding. Journal of Pharmacology and Experimental Therapeutics. 1992; 260(1):427-36

[9] Tejani-Butt S.M., Yang J., Zaffar H. Norepinephrine transporter sites are decreased in the locus coeruleus in Alzheimer's disease. Brain Res. 1993; 631(1):147-50

[10] Fitzgerald P.J. Is Elevated Norepinephrine an Etiological Factor in Some Cases of Alzheimers Disease? Current Alzheimer research. 2010; 7(6):506-16

[11] Gulyás B., Brockschnieder D., Nag S., Pavlova E., Kása P., Beliczai Z., Légrádi A., Gulya K., Thiele A., Dyrks T., Halldin C. The norepinephrine transporter (NET) radioligand (S,S)-[^{18}F]FMeNER-D_2 shows significant decreases in NET density in the human brain in Alzheimer's disease: a post-mortem autoradiographic study. Neurochemistry International. 2010; 56(6-7):789-98

[12] Delaville C., De Deurwaerdère P., Benazzouz A. Noradrenaline and Parkinson's Disease. Front Syst Neurosci. 2011; 5:31

[13] Curatolo P., D'Agathi E., Moavero R. The neurobiological basis of ADHD. Italian Journal of Pediatrics. 2010; 36:79

[14] Vanicek T., Spies M., Rami-Mark Ch., Savli M., Höflich A., Kranz G. S., Hahn A., Kutzelnigg A., Traub-Weidinger T., Mitterhauser M., Wadsak W., Hacker M., Volkow N.D., Kasper S., Lanzenberger R. The Norepinephrine Transporter in Attention-Deficit/Hyperactivity Disorder Investigated With Positron Emission Tomography. JAMA Psychiatry. 2014; 71(12):1340–1349

[15] Klimek V., Stockmeier C., Overholser J., Meltzer H.Y., Kalka S., Dilley G., Ordway G.A. Reduced Levels of Norepinephrine Transporters in the Locus Coeruleus in Major Depression. J Neurosci. 1997; 17:8451-8458

[16] Moret C., Briley M. The importance of norepinephrine in depression. Neuropsychiatr Dis Treat. 2011; 7(Suppl 1):9–13.

[17] Zhao Z., Zhang H-T., Bootzin E., Millan M.J., O'Donnell J.M. Association of Changes in Norepinephrine and Serotonin Transporter Expression with the Long-Term Behavioral Effects of Antidepressant Drugs. Neuropsychopharmacology. 2009 May; 34(6):1467–1481

[18] Ressler K., Nemeroff Ch. Role of norepinephrine in the pathophysiology of neuropsychiatric disorders. CNS Spectrums. 2001; 6(8):663-6, 670

[19] Miller D.K., Wong E.H.F., Dathan Chesnut M., Dwoskin L.P. Reboxetine: Functional Inhibition of Monoamine Transporters and Nicotinic Acetylcholine Receptors. JPET. 2002; 302:687-695

[20] Wong E.H.F., Ahmed S., Marshall R.C., McArthur R., Taylor D.P., Birgerson L., Cetera P. Highly selective Norepinephrine reuptake inhibitors and methods of using the same. WO. 2000; 01/01973

[21] Zheng G., Xue W., Wang P., Yang F., Li B., Li X., Li Y., Yao X., Zhu F. Exploring the Inhibitory Mechanism of Approved Selective Norepinephrine Reuptake Inhibitors and Reboxetine Enantiomers by Molecular Dynamics Study. Scientific Reports. 2016; 6:26883

[22] Zeng F., Jarkas N., Stehouwer J.S., Voll R.J., Owens M. J., Kilts C. D., Nemeroff Ch. B., Goodman M.M. Synthesis, in vitro characterization, and radiolabeling of reboxetine analogs as potential PET radioligands for imaging the norepinephrine transporter. Bioorganic & medicinal chemistry. 2008; 16(2):783-93

[23] Takano A., Gulyás B., Varrone A., Karlsson P., Schou M., Airaksinen A.J., Vandenhende F., Tauscher J., Halldin Ch. Imaging the norepinephrine transporter with positron emission tomography: initial human studies with (*S,S*)-[^{18}F]FMeNER-D_2. Eur J Nucl Med Mol Imaging. 2008; 35:153–157

[24] Rami-Mark Ch., Zhang M.R., Mitterhauser M., Lanzenberger R., Hacker M., Wadsak W. [^{18}F]FMeNER-D_2: Reliable fully-automated synthesis for visualization of the norepinephrine transporter. Nucl Med Biol. 2013; 40(8):1049–1054.

[25] Motulsky H. The GraphPad Guide to Analyzing Radioligand Binding Data. GraphPad Software. Copyright © 1995-96; http://www.graphpad.com (19.03.2015; 08.12.2017)

[26] Cheng Y., Prusoff W.H. Relationship between the inhibition constant (K1) and the concentration of inhibitor which causes 50 per cent inhibition (I50) of an enzymatic reaction. Biochem Pharmacol. 1973; 22:3099-108

[27] Reith M.E.A., Wang L.C., Dutta A. Pharmacological profile of radioligand binding to the norepinephrine transporter: Instances of poor indication of functional activity. Journal of Neuroscience Methods. 2005; 143(1):87-94

[28] Cheetham S. C., Viggers J. A., Butler S. A., Prow M. R., Heal D. J. [^{3}H]nisoxetine: a radioligand nodranenaline reuptake sites: correlation with inhibition of [^{3}H]norarenaline uptake and effect of DSP-4 lesioning and antidepressant treatments. Neuropharmacology. 1996; 35:63-70

[29] Keen M. Methods in Molecular Biology Volume 106. Receptor Binding Techniques. 1999, 3-23. Humana Press Inc.

[30] Brandel®. Harvester Operation and Service Manual. Brandel®, Inc. 2015

[31] Borai E. H., Lasheen Y. F., Seliman A. F., Abo-Aly M. M. Assessment of Quench Indicating Parameters (QIP) of an Alternative Scintillation Cocktail Mixture by Low Level Liquid Scintillation Counting. World Journal of Chemistry. 2007; 2(1):01-09

[32] Cherry S. R., Sorensen J. A., Phelps M.E. Physics in nuclear medicine. 2012; third ed., Elsevier Saunders

[33] Wang C. H., Willis D. L. Radiotracer Methodology in Biological Science. 1965. Prentice-Hall Inc.

[34] Kessler M. J. Liquid Scintillation Analysis. In: LSA Manual Science and technology. 2015; Perkin Elmer Inc®

[35] Kessler M. J. Liquid Scintillation Analysis. In: Handbook of Radioactivity Analysis. L' Annunziata M.F. 2012; third ed., Elsevier Inc.

[36] Perkin Elmer HIDEX 300SL brochure. HIDEX Oy; 2015

[37] Mark Ch., Bornatowicz B., Mitterhauser M., Hendl M., Nics L., Haeusler D., Lanzenberger R., Berger M.L., Spreitzer H., Wadsak W. Development and automation of a novel NET-PET tracer: [11C]Me@APPI. Nuclear Medicine and Biology. 2012; 40(2)

[38] Neudorfer C., Seddik A., Shanab K., Jurik A., Rami-Mark Ch., Holzer W., Ecker G., Mitterhauser M., Wadsak W., Spreitzer H. Synthesis and in Silico evaluation of novel compounds for PET-based investigations of the Noreinephrine Transporter. Molecules. 2015; 20:1712-1730

[39] Rami-Mark Ch., Berroteran-Infante N., Philippe C., Foltin St., Vraka Ch., Hoepping A., Lanzenberger R., Hacker M., Mitterhauser M., Wadsak W. Radiosynthesis and first preclinical evaluation of the Novel Norepinephrine Transporter PET-ligand [^{11}C]Me@HAPTHI. EJMMNI Research. 2015; 5:34

[40] Dumanic M., Li X., Rami-Mark Ch., Berroteran-Infante N., Philippe C., Vraka Ch., Wadsak W., Hacker M., Mitterhauser M. Evaluation of the cardiac neuronal function after acute myocardial infarction in rats using [^{11}C]Me@HAPTHI, a novel [^{11}C]-labeled PET tracer for the norepinephrine transporter. J Nucl Med. 2016; vol. 57 no. supplement 2 400

10 Abstract

The norepinephrine transporter (NET) has been involved to a multitude of neurological, psychiatric and cardiovascular pathologies over the last decade. Morbus Parkinson, Alzheimer's disease, major depression and the attention deficit hyperactivity disorder (ADHD) are the main maladies of an overabundance of NE reuptake. The appearance of these multiple disorders may be discovered prematurely with non-invasive molecular imaging techniques, such as positron emission tomography (PET). Therefore, appropriate PET-tracers with high affinity to NET are needed for clinical diagnostics.

The aim of this investigation was the screening of multiple compounds with different chemical structures for the illustration of novel suitable PET-tracers. Therefore, affinity test in vitro was chosen.

Radiolabelled binding assays with [^{3}H]Nisoxetine for NET display proper conditions for the elucidation of affinity and selectivity. Competition tests of radioactive ligands, non-specific binding ligands and new compounds were experimented using human NET expressing membranes. The consideration of right buffer composition, incubation times and temperature were contributory factors.

The Brandel® Cell Harvester Method for the filtration and collection of radiolabelled membranes were methods of choice. The measurement was terminated with the liquid scintillation analysis and completed with the analysis of specific binding with the GraphPad Prism Software. For the calculation of Ki values, the equation from Cheng and Prusoff was essential.

The conclusion of the experiments is, that five compounds demonstrate significant affinity and selectivity to NET: FAPPI 1, PHOXI 1, PHOXI 2, Me@DIMAP and Me@HAPTHI demonstrate Ki values ≤10nM.

Especially Me@HAPTHI evinced high affinity (Ki 0.2nM ± 0.06), that is the reason for the set up as ^{11}C-labelled ligand for preclinical experimentations.

11 Zusammenfassung

Der NA-Transporter hat sich als Hauptanteil von neurologischen, psychischen und kardiovaskulären Ursachen im letzten Jahrzehnt herausgestellt. Morbus Parkinson, Alzheimer, Depression und das Aufmerksamkeitsdefizit-Hyperaktivitätssyndrom entstehen durch übermäßige Wiederaufnahme von Noradrenalin. Für eine Früherkennung dieser Erkrankungen sind nicht invasive bildgebende Techniken wie PET erforderlich. Aus diesem Grund sind passende PET-tracer mit hoher Affinität zum Noradrenalin-Transporter für die klinische Diagnostik erforderlich.

Ziel dieser Arbeit war es, Voruntersuchungen verschiedener Verbindungen mit unterschiedlicher chemischer Struktur für die Verwendung als PET-Tracer durchzuführen. Methode der Wahl war die in-vitro Affinitätsbindungsstudie.

Besonders geeignet für die Evaluierung von Affinität und Selektivität war die kompetitive Bindungsstudie mit radioaktivmarkierte [^{3}H]Nisoxetin. Die Inhibitionstests wurden jeweils mit radioaktivem Liganden, Referenz und neuer Substanzen an Membranen, die humane NA-transporter exprimieren, durchgeführt. Dabei wurden die richtige Pufferzusammensetzung, die Inkubationszeit und die Temperatur als begrenzende Faktoren beachtet.

Zur Filtration und Sammlung der markierten Membranen wurde die Zellsammlungsmethode von Brandel® [30] gewählt. Für die Messung der Radioaktivität eignete sich die Flüssig-Szintillationszählung, deren Auswertung mittels GraphPad Prism Software erfolgte. Für die Berechnung der Ki-Werte war die Formel von Cheng und Prusoff [26] erforderlich.

Zusammenfassend weisen fünf der getesteten Verbindungen hohe Affinität und Selektivität am NA-Transporter vor: FAPPI 1, PHOXI 1, PHOXI 2, Me@DIMAP und Me@HAPTHI zeigen Ki-Werte ≤10nM.

Hervorzuheben ist die höchste Affinität von Me@HAPTHI am NA-Transporter mit einem Ki-Wert von 0,2nM ± 0,06. Aus diesem Grund werden bereits weitere präklinische Studien mit dem ^{11}C-markierten Liganden untersucht.

12 Appendix

12.1 Tables

12.2 Figures

12.3 List of abbreviations

AD	Alzheimer`s disease
AKH	Allgemeines Krankenhaus, general hospital
ATX	Atomoxetine
cAMP	Cyclic adenosine monophosphate
COMT	Catechol-O-methyl transferase
CPM	Counts per minute
DAT	Dopamine transporter
DA	Dopamine
DIMAP	“Dimethylinodlin-amino-propan”
DHPG	3,4-dihydroxyphenylglycol
DOPA	Dopamine
DPM	Disintegrations per minute
DS	Desimipramine
EMT	Extraneuronal monoamine transporter
ERK	Extracellular signal regulated kinase
FAPPI	“Fluorphenyl-methylamino-propyl-phenyl-dihydro-imidazol”
HAPTHI	“Hydroxy-amino-propyl-phenyl-thiadiazol”
IC50	Half maximal inhibitory concentration
Ki	Inhibition potency
LC	Locus coeruleus
MAO	Monoamine oxidase
MAPK	Mitogen acitvated protein kinase
MAPPI	“Methylamino-phenylproopyl-indolin”
MHPG	3-hydroxy-4-methoxyphenylglycol
MPH	Methylphenidate
MV	Mean value
NE	Norepinephrine

NET	Norepinephrine transporter
NIS	Nisoxetine
NRI	Norepinephrine reuptake inhibitor
nM	Nanomolar
n.v.	No values
RBX	Reboxetine
PEI	Polyethylenimin
PET	Positron emission tomography
PHOXI	“Phenoxyisochromen”
PMT	Photomultiplier tube
PNMT	Phenylethanolamine N-methyltransferase
Ras	Rat sarcoma
SDS-Page	Sodium dodecyl sulfate polyacrylamide gel electrophoresis
SERT	Serotonin transporter
sNRI	Selective Norepinephrine reuptake inhibitor
STD	Standard deviation
TCA	Tricyclic antidepressants
TDCR	Triple-to-double coincidence ratio
TRIS	Tris(hydroxymehtyl)-aminomethan
VAM	Vanillylmandelic acid
VMAT	Vesicular monoamine transporter
5-HT	5-Hydroxitryptamine, Serotonin

12.4 Technical data sheets

12.4.1 Membrane Target Systems™

TECHNICAL DATA SHEET

Membrane Target Systems™

Caution: For Laboratory Use. A research reagent for research purposes only

human Norepinephrine Transporter

Product No.: RBHNETM400UA

Lot No.: 1908437

Material Provided

Membranes:	1 x 400 units / 400 µL frozen aliquot

Product Information

Cellular Background:	MDCK
GenBank Accession Number:	NM_001043
Unit Size:	3 µg protein / unit
Storage Buffer:	50 mM Tris-HCL (pH 7.4), 0.5mM EDTA, 10mM $MgCl_2$, 10% sucrose.
Storage Conditions:	Store at -80°C. **Freeze-thaw is not recommended** as it can affect product performance and homogeneity. In order to minimize negative impact of freeze-thawing, flash freeze in liquid nitrogen for 30 seconds prior to transferring to -80°C.
Stability:	This product is stable for at least 3 years from reception if used and stored under recommended conditions.

Quality Control

Bmax and Kd are determined using radioactive saturation binding assays (Figure 1). Protein concentration is determined using the BCA method [1]. Ratio-to-Reference (RTR) is determined by dividing the maximal signal of the current lot (Bmax in fmoles) by the maximal signal of a pre-defined reference tested in parallel. RTR is an indicator of lot-to-lot consistency. *We certify that these results meet our quality release criteria.

Ratio-to-Reference (RTR):	NA
Expression Level (B_{MAX}):	15.3 pmol/mg membrane protein.
K_D for [^{3}H]-Nisoxetine :	3.29 nM
Protein Concentration:	3 µg/µL

*(1) Smith, P.K., et al. (1985). Anal. Biochem. **150**, 76-85.*

PerkinElmer
For the Better

Recommended Assay Conditions

Assay Buffer: 50 mM Tris-HCl pH 7.4, 120 mM NaCl, 5 mM KCl

Wash Buffer: 50 mM Tris-HCl pH 7.4, 154 mM NaCl

Binding Protocol: Binding assays are performed in 550 µL total volume according to the following conditions:

1 - Membrane dilution: 0.05 mL of membranes + 24.95 mL assay buffer (1:500 dilution)

2 - Incubation: 25 µL of incubation buffer or Desipramine (Sigma D3900) 1 µM final for non specific binding (Saturation binding assay)

For competition binding assay: 25 µL of reference compounds at decreasing concentrations (see figure 2)

25 µL of radioligand at the appropriate concentration (see graph below)
500 µL of diluted membranes

3 - Incubation time: 60 minutes at 4 °C

4 - Filtration: aspirate and wash 9 x 500 µL with ice cold wash buffer over GF/C filter (presoaked in 0.5 % PEI).

Lot Specific Data

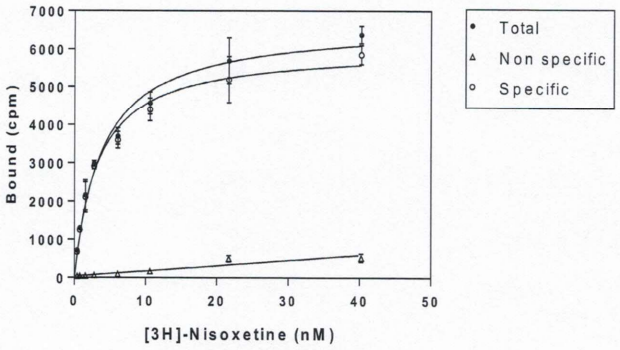

Figure 1: Saturation binding assay curve (filtration)
96-well saturation binding assay curve (3 µg membranes/well, TopCount®) using [^{3}H]-Nisoxetine (PerkinElmer NET1084 Lot No.:1863950)

PerkinElmer
For the Better

Typical Product Data

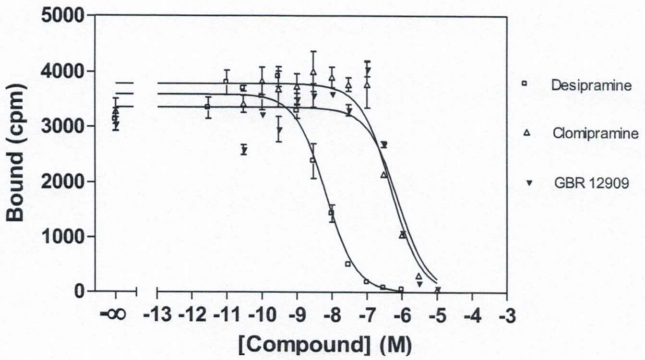

Figure 2: Competition binding assay curve (filtration)
96-well competition binding assay curve (3 µg membranes/well, TopCount®). Recommended radioligand concentration = 4 nM.

*Even though two sites can be observed occasionally with some ligands, the data presented is derived from single site fitting.

Reference Compounds	Ki (nM)
Desipramine	3.2
Clomipramine	235
GBR 12909	373

PerkinElmer
For the Better

Suggested Materials and Instrumentation

Please visit our website

www.perkinelmer.com/GPCR

This product is not for resale or distribution except by authorized distributors.

LIMITED WARRANTY: PerkinElmer BioSignal Inc. warrants that, at the time of shipment, the products sold by it are free from defects in material and workmanship and conform to specifications which accompany the product. PerkinElmer BioSignal Inc. makes no other warranty, express or implied with respect to the products, including any warranty of merchantability or fitness for any particular purpose. Notification of any breach of warranty must be made within 60 days of receipt unless otherwise provided in writing by PerkinElmer BioSignal Inc. No claim shall be honored if the customer fails to notify PerkinElmer BioSignal Inc. within the period specified. The sole and exclusive remedy of the customer for any liability of PerkinElmer BioSignal Inc. of any kind including liability based upon warranty (express or implied whether contained herein or elsewhere), strict liability contract or otherwise is limited to the replacement of the goods or the refunds of the invoice price of goods. PerkinElmer BioSignal Inc. shall not in any case be liable for special, incidental or consequential damages of any kind.

PerkinElmer, Inc.
940 Winter Street
Waltham, MA 02451 USA
P: (800) 762-4000 or
(+1) 203-925-4602
www.perkinelmer.com

PerkinElmer®

For a complete listing of our global offices, visit www.perkinelmer.com/ContactUs

TECHNICAL DATA SHEET

Membrane Target Systems™

Caution: For Laboratory Use. A research reagent for research purposes only

human Dopamine Transporter

Product No.: RBHDATM400UA

Lot No.: 1696714

Material Provided

Membranes: 1 x 400 units / 400 µL frozen aliquot

Product Information

Cellular Background: CHO-K1

GenBank Accession Number: NM_001044

Unit Size: 12 µg protein / unit

Storage Buffer: 50 mM Tris-HCL (pH 7.4), 0.5mM EDTA, 10mM $MgCl_2$, 10% sucrose.

Storage Conditions: Store at -80°C. **Freeze-thaw is not recommended** as it can affect product performance and homogeneity. In order to minimize negative impact of freeze-thawing, flash freeze in liquid nitrogen for 30 seconds prior to transferring to -80°C.

Stability: This product is stable for at least 3 years from reception if used and stored under recommended conditions.

Quality Control

Bmax and Kd are determined using radioactive saturation binding assays (Figure 1). Protein concentration is determined using the BCA method [1]. Ratio-to-Reference (RTR) is determined by dividing the maximal signal of the current lot (Bmax in fmoles) by the maximal signal of a pre-defined reference tested in parallel. RTR is an indicator of lot-to-lot consistency. *We certify that these results meet our quality release criteria.

Ratio-to-Reference (RTR): 0.54

Expression Level (B_{MAX}): 5.0 pmol/mg membrane protein.

K_D for [^{3}H]-WIN 35,428 : 23.8 nM

Protein Concentration: 12 µg/µL

(1) *Smith, P.K., et al. (1985). Anal. Biochem.* ***150****, 76-85.*

PerkinElmer
For the Better

Recommended Assay Conditions

Assay Buffer: 50 mM Tris-HCl pH 7.4, 100 mM NaCl

Wash Buffer: 50 mM Tris-HCl pH 7.4, 100 mM NaCl

Binding Protocol: Binding assays are performed in 550 µL total volume according to the following conditions:

1 - Membrane dilution: 0.05 mL of membranes + 24.95 mL assay buffer (1: 500 dilution)

2 - Incubation: 25 µL of incubation buffer or GBR 12909 (Sigma D052) 10 µM final for non specific binding (Saturation binding assay)

For competition binding assay: 25 µL of reference compounds at decreasing concentrations (see figure 2)

25 µL of radioligand at the appropriate concentration (see graph below)
500 µL of diluted membranes

3 - Incubation time: 120 minutes at 4 °C

4 - Filtration: aspirate and wash 9 x 500 µL with ice cold wash buffer over GF/C filter (presoaked in 0.5 % PEI).

Lot Specific Data

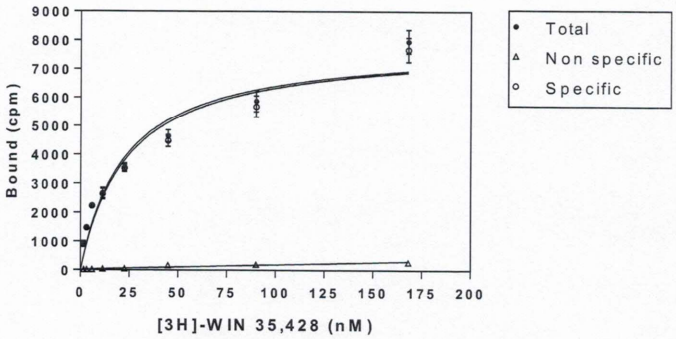

Figure 1: Saturation binding assay curve (filtration)
96-well saturation binding assay curve (12 µg membranes/well, TopCount®) using [^{3}H]-WIN 35,428 (PerkinElmer NET1033 Lot No.: 1783740)

PerkinElmer
For the Better

Typical Product Data

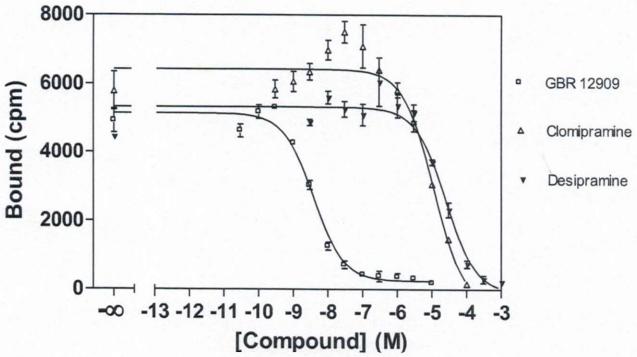

Figure 2: Competition binding assay curve (filtration)
96-well competition binding assay curve (12 µg membranes/well, TopCount®). Recommended radioligand concentration = 25 nM.

*Even though two sites can be observed occasionally with some ligands, the data presented is derived from single site fitting.

Reference Compounds	Ki (nM)
GBR 12909	1.5
Clomipramine	4369
Desipramine	9850

PerkinElmer®
For the Better

Suggested Materials and Instrumentation

Please visit our website

www.perkinelmer.com/GPCR

This product is not for resale or distribution except by authorized distributors.

LIMITED WARRANTY: PerkinElmer BioSignal Inc. warrants that, at the time of shipment, the products sold by it are free from defects in material and workmanship and conform to specifications which accompany the product. PerkinElmer BioSignal Inc. makes no other warranty, express or implied with respect to the products, including any warranty of merchantability or fitness for any particular purpose. Notification of any breach of warranty must be made within 60 days of receipt unless otherwise provided in writing by PerkinElmer BioSignal Inc. No claim shall be honored if the customer fails to notify PerkinElmer BioSignal Inc. within the period specified. The sole and exclusive remedy of the customer for any liability of PerkinElmer BioSignal Inc. of any kind including liability based upon warranty (express or implied whether contained herein or elsewhere), strict liability contract or otherwise is limited to the replacement of the goods or the refunds of the invoice price of goods. PerkinElmer BioSignal Inc. shall not in any case be liable for special, incidental or consequential damages of any kind.

PerkinElmer, Inc.
940 Winter Street
Waltham, MA 02451 USA
P: (800) 762-4000 or
(+1) 203-925-4602
www.perkinelmer.com

PerkinElmer®

For a complete listing of our global offices, visit www.perkinelmer.com/ContactUs

TECHNICAL DATA SHEET

Membrane Target Systems™

Caution: For Laboratory Use. A research reagent for research purposes only

human Serotonin Transporter

Product No.: RBHSTM400UA

Lot No.: 1719066

Material Provided

Membranes:	1 x 400 units / 400 µL frozen aliquot

Product Information

Cellular Background:	HEK293
GenBank Accession Number:	NM_001045
Unit Size:	9 µg protein / unit
Storage Buffer:	50 mM Tris-HCL (pH 7.4), 0.5mM EDTA, 10mM $MgCl_2$, 10% sucrose.
Storage Conditions:	Store at -80°C. **Freeze-thaw is not recommended** as it can affect product performance and homogeneity. In order to minimize negative impact of freeze-thawing, flash freeze in liquid nitrogen for 30 seconds prior to transferring to -80°C.
Stability:	This product is stable for at least 3 years from reception if used and stored under recommended conditions.

Quality Control

Bmax and Kd are determined using radioactive saturation binding assays (Figure 1). Protein concentration is determined using the BCA method [1]. Ratio-to-Reference (RTR) is determined by dividing the maximal signal of the current lot (Bmax in fmoles) by the maximal signal of a pre-defined reference tested in parallel. RTR is an indicator of lot-to-lot consistency. *We certify that these results meet our quality release criteria.

Ratio-to-Reference (RTR):	N/A
Expression Level (B_{MAX}):	7.6 pmol/mg membrane protein.
K_D for [^{3}H]-Imipramine :	1.88 nM
Protein Concentration:	9 µg/µL

(1) Smith, P.K., et al. (1985). Anal. Biochem. ***150****, 76-85.*

PerkinElmer
For the Better

Recommended Assay Conditions

Assay Buffer: 50 mM Tris-HCl pH 7.4, 120 mM NaCl, 5 mM KCl

Wash Buffer: 50 mM Tris-HCl pH 7.4, 154 mM NaCl

Binding Protocol: Binding assays are performed in 550 µL total volume according to the following conditions:

1 - Membrane dilution:	0.05 mL of membranes + 24.95 mL assay buffer (1:500 dilution)
2 - Incubation:	25 µL of incubation buffer or Imipramine (Sigma I0899) 200 µM final for non specific binding (Saturation binding assay)
	For competition binding assay: 25 µL of reference compounds at decreasing concentrations (see figure 2)
	25 µL of radioligand at the appropriate concentration (see graph below) 500 µL of diluted membranes
3 - Incubation time:	30 minutes at 27 °C
4 - Filtration:	aspirate and wash 9 x 500 µL with ice cold wash buffer over GF/C filter (presoaked in 0.5 % PEI).

Lot Specific Data

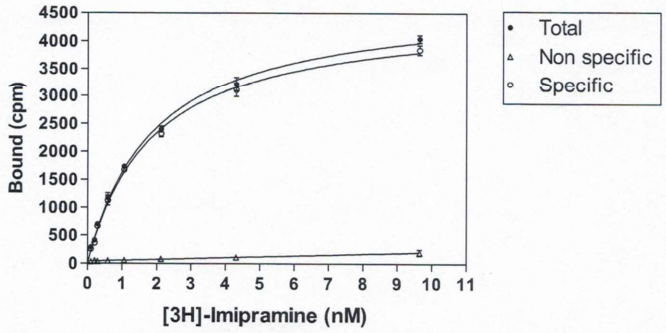

Figure 1: Saturation binding assay curve (filtration)
96-well saturation binding assay curve (9 µg membranes/well, TopCount®) using [^{3}H]-Imipramine (PerkinElmer NET576 Lot No.: 1587010)

PerkinElmer®
For the Better

Typical Product Data

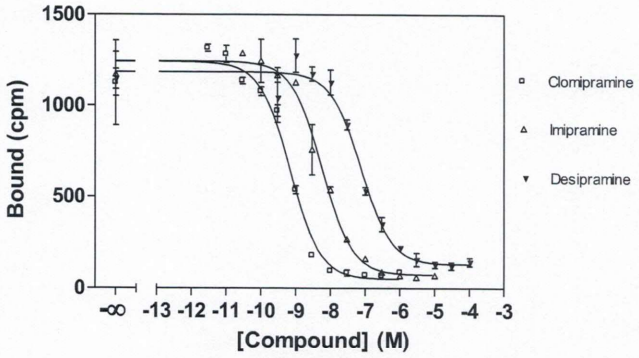

Figure 2: Competition binding assay curve (filtration)
96-well competition binding assay curve (9 µg membranes/well, TopCount®). Recommended radioligand concentration = 2 nM.

*Even though two sites can be observed occasionally with some ligands, the data presented is derived from single site fitting.

Reference Compounds	Ki (nM)
Clomipramine	0.53
Imipramine	4.4
Desipramine	57

PerkinElmer®
For the Better

Suggested Materials and Instrumentation

Please visit our website

www.perkinelmer.com/GPCR

This product is not for resale or distribution except by authorized distributors.

LIMITED WARRANTY: PerkinElmer BioSignal Inc. warrants that, at the time of shipment, the products sold by it are free from defects in material and workmanship and conform to specifications which accompany the product. PerkinElmer BioSignal Inc. makes no other warranty, express or implied with respect to the products, including any warranty of merchantability or fitness for any particular purpose. Notification of any breach of warranty must be made within 60 days of receipt unless otherwise provided in writing by PerkinElmer BioSignal Inc. No claim shall be honored if the customer fails to notify PerkinElmer BioSignal Inc. within the period specified. The sole and exclusive remedy of the customer for any liability of PerkinElmer BioSignal Inc. of any kind including liability based upon warranty (express or implied whether contained herein or elsewhere), strict liability contract or otherwise is limited to the replacement of the goods or the refunds of the invoice price of goods. PerkinElmer BioSignal Inc. shall not in any case be liable for special, incidental or consequential damages of any kind.

PerkinElmer, Inc.
940 Winter Street
Waltham, MA 02451 USA
P: (800) 762-4000 or
(+1) 203-925-4602
www.perkinelmer.com

PerkinElmer®

For a complete listing of our global offices, visit www.perkinelmer.com/ContactUs

12.4.2 Radioligands

TECHNICAL DATA SHEET ^{3}H

Caution: For Laboratory Use. A product for research purposes only.

NISOXETINE HCl, [N-METHYL-^{3}H]-

Product Number: NET1084

LOT SPECIFIC INFORMATION

Lot Number:	2021539
Specific Activity:	84.3 Ci/mmol
	3119 GBq/mmol
Production Date:	22 May 2015

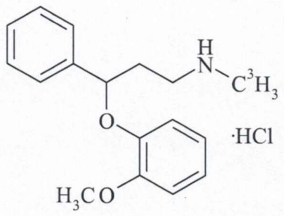

M.W. 307
$C_{17}H_{22}ClNO_2$

PACKAGING: 1 mCi/ml (37 MBq/ml) in ethanol, under argon. Shipped in dry ice.

STABILITY AND STORAGE RECOMMENDATIONS: When nisoxetine HCl, [N-methyl-^{3}H]- is stored at -20°C in its original solvent and at its original concentration, the initial rate of decomposition is approximately 1% for 6 months. Stability is nonlinear and not correlated to isotope half-life. Lot to lot variation may occur.

SPECIFIC ACTIVITY RANGE: 70-87 Ci/mmol (2590-3219 GBq/mmol)

RADIOCHEMICAL PURITY: This product was initially found to be greater than 97% when determined by the following method. The rate of decomposition can accelerate. Purity should be checked prior to use:

High pressure liquid chromatography on a Rx-C8 column using the following mobile phase:
1% triethylammonium acetate pH 4 : acetonitrile, (60:40).

QUALITY CONTROL: The radiochemical purity of nisoxetine HCl, [N-methyl-^{3}H]- is checked at appropriate intervals using the listed chromatography method.

REFERENCES:

1. D.T. Wong, J.S. Horng, and F.P. Bymaster, *Life Sci.*,17, 755 (1975).
2. S.M. Tejani-Butt, D.J. Brunswick, and A. Frazer, *Eur. J. Pharmacol.*, 191, 239 (1990).
3. S.M. Tejani-Butt, *J. Pharmacol. Exp. Ther.*, 260, 427 (1992).

HAZARD INFORMATION: WARNING: This product contains a chemical known to the state of California to cause cancer.

PerkinElmer, Inc.
549 Albany Street
Boston, MA 02118 USA
P: (800) 762-4000 or (+1) 203-925-4602
www.perkinelmer.com/nenradiochemicals
For a complete listing of our global offices, visit www.perkinelmer.com/ContactUs

PerkinElmer®

TECHNICAL DATA SHEET

^{3}H

Caution: For Laboratory Use. A product for research purposes only.

WIN 35,428, [N-METHYL-^{3}H]-

Product Number: NET1033

LOT SPECIFIC INFORMATION

Lot Number:	2027828	
Specific Activity:	82.62	Ci/mmol
	3056	GBq/mmol
Production Date:	04-Jun-2015	

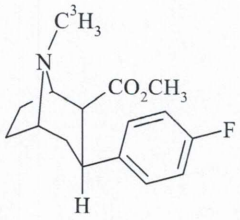

M.W. 277
$C_{16}H_{20}FNO_2$

PACKAGING: 1.0 mCi/ml (37 MBq/ml) in ethanol, under argon. Shipped in dry ice.

STABILITY AND STORAGE RECOMMENDATIONS: When WIN 35,428, [N-methyl-^{3}H]- is stored at -20°C in its original solvent and at its original concentration, the rate of decomposition is initially 3% for 6 months from date of purification. Stability is nonlinear and not correlated to isotope half-life. Lot to lot variation may occur.

SPECIFIC ACTIVITY RANGE: 60-87 Ci/mmol (2220-3219 GBq/mmol)

RADIOCHEMICAL PURITY: This product was initially found to be greater than 97% when determined by the following methods. The rate of decomposition can accelerate. It is advisable to check purity prior to use:

High pressure liquid chromatography on a Zorbax ODS column using the following mobile phase:
1% triethylamine acetate, pH 4 : methanol, (7:3).

QUALITY CONTROL: The radiochemical purity of WIN 35,428, [N-methyl-^{3}H]- is checked at appropriate intervals using the first listed chromatography method.

HAZARD INFORMATION: WARNING: This product contains a chemical known to the state of California to cause cancer.

PerkinElmer, Inc.
549 Albany Street
Boston, MA 02118 USA
P: (800) 762-4000 or (+1) 203-925-4602
www.perkinelmer.com/nenradiochemicals
For a complete listing of our global offices, visit www.perkinelmer.com/ContactUs

PerkinElmer®

TECHNICAL DATA SHEET

^{3}H

Caution: For Laboratory Use. A product for research purposes only.

IMIPRAMINE HYDROCHLORIDE, [BENZENE RING-^{3}H(N)]-

Product Number: NET576

LOT SPECIFIC INFORMATION

Lot Number:	2064485
Specific Activity:	51.6 Ci/mmol
	1909 GBq/mmol
Production Date:	28 Aug 2015

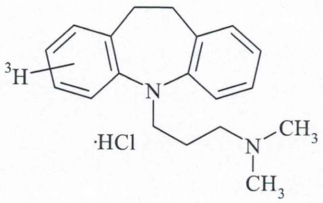

M.W. 316
$C_{19}H_{25}ClN_2$

PACKAGING: 1.0 mCi/ml (37 MBq/ml) in ethanol, under argon, in a vial which protects the contents from UV light. Shipped on dry ice.

STABILITY AND STORAGE RECOMMENDATIONS: When imipramine hydrochloride, [benzene ring-^{3}H(N)]- is stored at -20°C in its original solvent and at its original concentration, the rate of decomposition is initially 0.5% per month from date of purification. Stability is nonlinear and not correlated to isotope half-life. Lot to lot variation may occur.

SPECIFIC ACTIVITY RANGE: 40-70 Ci/mmol (1480-2590 GBq/mmol)

RADIOCHEMICAL PURITY: This product was initially found to be greater than 97% when determined by the following methods. The rate of decomposition can accelerate. It is advisable to check purity prior to use:

High pressure liquid chromatography on a Zorbax CN column using the following mobile phase:
1% triethylammonium acetate pH4 : acetonitrile, (9:1).

Thin layer chromatography on silica gel using the following solvent systems:
a. chloroform : methanol : ammonium hydroxide, (9:1:0.1).
b. ethanol : ammonium hydroxide, (29:1).
c. ethyl acetate : butanol : ethanol : ammonium hydroxide, (70:10:15:1).

QUALITY CONTROL: The radiochemical purity of imipramine hydrochloride, [benzene ring-^{3}H(N)]- is checked at appropriate intervals using the first listed chromatography method.

HAZARD INFORMATION: WARNING: This product contains a chemical known to the state of California to cause cancer.

PerkinElmer, Inc.
549 Albany Street
Boston, MA 02118 USA
P: (800) 762-4000 or (+1) 203-925-4602
www.perkinelmer.com/nenradiochemicals
For a complete listing of our global offices, visit www.perkinelmer.com/ContactUs

PerkinElmer®